Hydrogeology Journal
DOI 10.1007/s10040-014-1219-9

Groundwater conceptualization and modeling using distributed SWAT-based recharge for the semi-arid agricultural Neishaboor plain, Iran

A. Izady · K. Davary · A. Alizadeh · A. N. Ziaei · S. Akhavan · A. Alipoor · A. Joodavi · M. L. Brusseau

Abstract Increased irrigation in the Neishaboor watershed, Iran, during the last few decades has caused serious groundwater depletion, making the development of comprehensive mitigation strategies and tools increasingly important. In this study, SWAT and MODFLOW were employed to integratively simulate surface-water and groundwater flows. SWAT and MODFLOW were iteratively executed to compute spatial and temporal distributions of hydrologic components. The combined SWAT-MODFLOW model was calibrated (2000–2010) and validated (2010–2012) based on streamflow, wheat yield, groundwater extraction, and groundwater-level data. This multi-criteria calibration procedure provided greater confidence for the partitioning of water between soil storage, actual evapotranspiration, and aquifer recharge. The SWAT model provided satisfactory predictions of the hydrologic budget for the watershed outlet. It also provided good predictions of irrigated wheat yield and groundwater extraction. The 10-year mean annual recharge rate estimated using the combined model varied greatly, ranging from 0 to 960 mm, with an average of 176 mm. This result showed good agreement with the independently estimated annual recharge rate from an earlier study. The combined model provides a robust tool for the sustainable planning and management of water resources for areas with stressed aquifers where interaction between groundwater and surface water cannot be easily assessed.

Keywords Groundwater/surface-water relations · Groundwater recharge/water budget · Over-abstraction · Combined calibration · Iran

Received: 18 February 2013 / Accepted: 25 November 2014

Electronic supplementary material The online version of this article (doi:10.1007/s10040-014-1219-9) contains supplementary material, which is available to authorized users.

A. Izady · K. Davary · A. Alizadeh · A. N. Ziaei
Water Engineering Department, College of Agriculture, Ferdowsi University of Mashhad, Mashhad, Iran

S. Akhavan
Water Engineering Department, College of Agriculture, Bu-Ali Sina University, Hamadan, Iran

A. Alipoor
Neishaboor Water Authority, Neishaboor, Iran

A. Joodavi
Earth Sciences Department, College of Sciences, Shiraz University, Shiraz, Iran

A. Izady (✉) · M. L. Brusseau
Soil, Water and Environmental Science Department, University of Arizona, Tucson, AZ, USA
e-mail: az.izady@gmail.com

Introduction

Due to over exploitation of aquifers, many regions of the world (e.g. Middle East and North Africa, India, China, Japan and Spain) face critical water-resource sustainability issues (Llamas and Custodio 2002). Groundwater in the Neishaboor plain in Iran has significant socioeconomic importance, both as a factor of production in agriculture and as a source of drinking water. During the past few decades, this aquifer has experienced severe groundwater depletion and overexploitation which has resulted in the general prohibition, since 1986, of any further development in this area (Hoseini et al. 2005). There are many unauthorized wells in the plain and pumping is not regulated, resulting in over-exploitation of the aquifer, which has caused an approximate annual groundwater level decline of 1 m in recent years. Moreover, recent studies have revealed an increasing trend in long-term mean annual precipitation, as well as more quickly increasing trend in evapotranspiration (Ghahraman 2006; Ghahraman and Taghvaeian 2008). This has resulted in an increase in irrigation water required to support agriculture, providing additional demand for groundwater. More conflicts and complexities are bound to occur within the region, unless an integrated water-resources management program is put into action. Such a program must be based on a sound understanding of the hydrological system, and employ robust modeling tools to better support decision making.

The comprehensive recognition and proper management of valuable groundwater resources, especially in arid and semi-arid areas, has an important influence on the

Published online: 11 December 2014

sustainable development of social and economic activities (Izady et al. 2012, 2013). During recent decades, disputes have occurred among water users for the rights to groundwater, particularly in highly exploited areas. The lack of knowledge about groundwater behavior and of the availability of the resource precludes the formulation of suitable groundwater management plans. The use of mathematical modeling to simulate groundwater behavior can enhance understanding of aquifer conditions and resource availability (e.g., Bredehoeft and Hall 1995; Bedekar et al. 2012; Doherty and Simmons 2013).

Recharge has a crucial role in groundwater modeling, especially in arid and semi-arid areas (Scanlon et al. 2002; De Vries and Simmers 2002; Sophocleous 2005; Scanlon et al. 2006; Wheater 2010; Herczeg and Leaney 2011). Unless accurate recharge rates are provided, the impacts of withdrawing groundwater from an aquifer cannot be properly assessed, and the long-term behavior of an aquifer under various management scenarios cannot be reliably estimated (Sophocleous 2005).

A wide variety of techniques is available for quantifying groundwater recharge in arid and semi-arid areas. The problem of estimating groundwater recharge in these areas is that recharge amounts are normally small in comparison with the resolution of the investigation methods (Allison et al. 1984). Direct groundwater recharge from precipitation is also generally small, usually less than about 5 % of the average annual precipitation, with a high temporal and spatial variability (Gieske 1992; Wheater 2010). Lerner et al. (1990) pointed out that determination of groundwater recharge in arid and semi-arid areas is neither straightforward nor easy. This is generally due to the spatial variability in soil characteristics, geology, topography, land cover characteristics and land use; and moreover, a consequence of the temporal variability of precipitation and other hydrometeorological variables in such climates. As a result of these factors, generating the recharge data required as input to modeling groundwater flow is difficult and complex. As a result, there is considerable uncertainty in the simulated groundwater flow results (Kim et al. 2008).

Scanlon et al. (2002) concluded that models play a very useful role in the recharge estimation process because of the ability to consider the impact of many different parameters on recharge. Also, they are used to assess conceptual models, to determine the sensitivity of recharge estimates to various parameters, and to predict how future changes in climate and land use may affect recharge rates. Therefore, the use of models to estimate recharge is an attractive option for arid and semi-arid areas. Among existing models in the literature, SWAT (Arnold et al. 1998) has been shown to be a generally robust model (Sophocleous et al. 1999; Sophocleous and Perkins 2000; Sun and Cornish 2005; Bejranonda et al. 2007; Kim et al. 2008). Sun and Cornish (2005) suggested that a catchment-based approach as is done with SWAT is needed for recharge estimation on a catchment scale. Point-scale models have their value in improving understanding of processes, but care is needed when extrapolating to large catchments without some observed data at the catchment scale to limit the estimation error. SWAT was developed for assessing the impact of management and climate on water supplies, sediment, and agricultural chemical yields in watersheds and larger river basins. It is a semi-distributed, time continuous watershed simulator operating on a daily time step. The major components of SWAT comprise hydrology, weather, plant growth, land management, and stream routing. Since crop yield is directly proportional to actual evapotranspiration (Jensen 1968; FAO 1986), calibration of SWAT using crop yield in addition to streamflow provides greater confidence for the partitioning of water between soil storage, actual evapotranspiration, and aquifer recharge (Srinivasan et al. 2010; Nair et al. 2011).

The principle objective of this study was to simulate groundwater behavior in the Neishaboor plain to support water-resources decision making. The combined SWAT-MODFLOW model is used to estimate groundwater recharge. Furthermore, transient groundwater flow modeling has been undertaken to complement and confirm the findings of the recharge estimation method.

Material and methods

Study area

The study area is the Neishaboor watershed, which is located between 35°40′ N to 36°39′ N latitude and 58°17′ E to 59°30′ E longitude in the northeast of Iran (Fig. 1). The total area is 9,158 km^2 and consists of 4,241 km^2 mountainous terrains and about 4,917 km^2 of plain. The maximum elevation is located in Binalood Mountains (3,300 m above sea level), and the minimum elevation is at the outlet of the watershed (Hoseinabad) at 1,050 m above sea level. The average daily discharge at Hoseinabad station was 0.36 m^3/s for the period of 1997–2010, with a minimum value of zero and a maximum value of 89 m^3/s. The area has a semi-arid to arid climate, with an average annual precipitation of 265 mm that varies considerably from one year to another (Coefficient Variation; CV=0.13). The mean annual temperatures changes from 13 ° C at Bar station (in the mountainous area) to 13.8 °C at Fedisheh station (in the plain area). The annual potential evapotranspiration is about 2,335 mm (Velayati and Tavassloi 1991).

The largest riparian zone is associated wtih Maroosk River, which is approximately 500 m in width. Major alluvial fans are located south of Kharv (the area is approximately 36 km^2). Moreover, several alluvial plains are located in the Mirabad area (north of Neishaboor city), with a combined area of about 27 km^2, and in northern areas of the study area (such as Bujan, Grineh, Maroosk, etc.) for which the combined area is about 40–50 km^2. The alluvium in the central section of the plain is comprised of silt and clay-sized grains. These fine-grained alluviums have undergone salinization near the

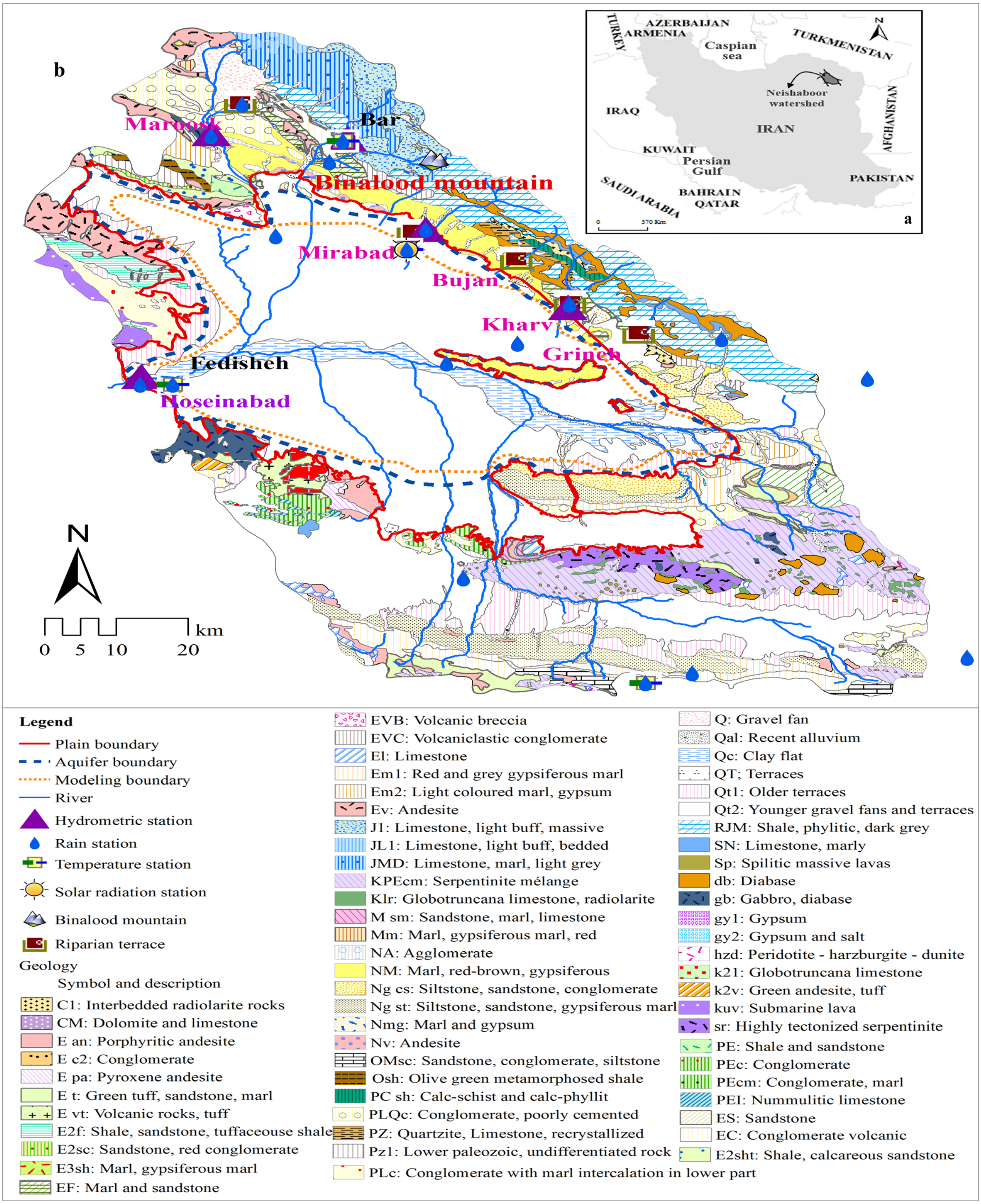

Fig. 1 **a** Neishaboor watershed location map, **b** Geological map along with plain, aquifer and modeling boundaries, meteorological stations and river network of the Neishaboor watershed

plain's outlet due to past evaporation of groundwater (Velayati and Tavassloi 1991).

The regional groundwater flow originates primarily from the east, northeast and south and discharges to the

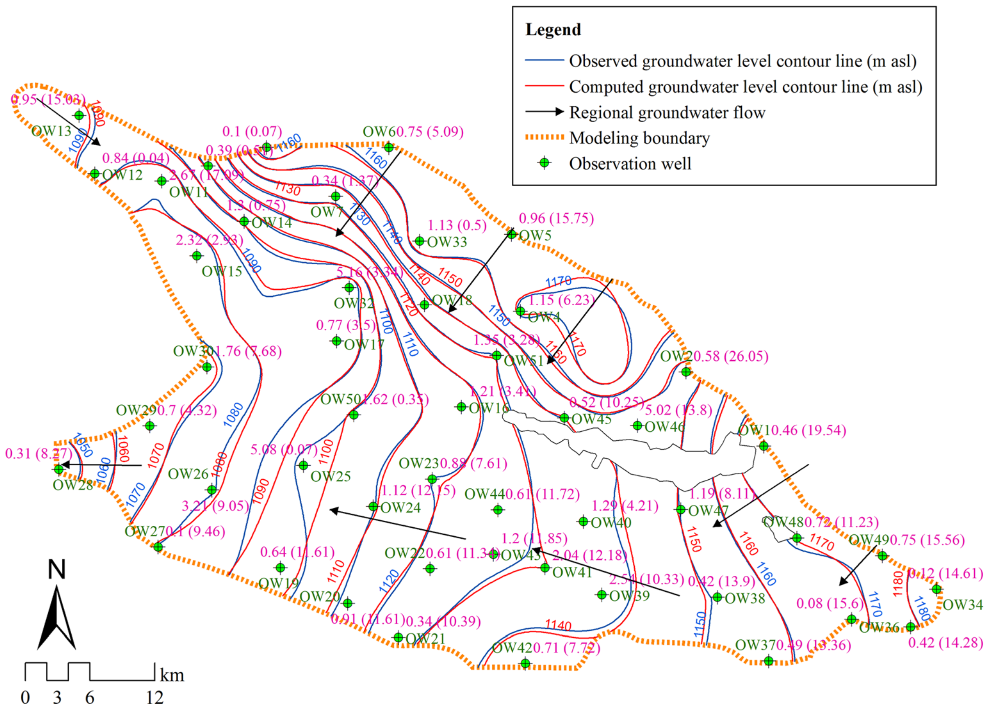

Fig. 2 Observed (*blue line*) and computed (*red line*) groundwater level contour lines for the Neishaboor aquifer (Oct. 2010) along with regional groundwater flow direction (m asl is meters above sea level). The starting date of the calibration period is 1 Oct. 2000. Observation well names are given in *green*; *numbers* beside observation wells (*in purple*) are RMSE performance criteria and groundwater level fluctuation of each observation well (*in parenthesis*; units in meters)

southwest of the study area (Fig. 2). Fluctuations in groundwater levels were classified into three categories. In the first category located in the northwest of the plain, the water-table fluctuations are small due to receipt of considerable amounts of recharge and significant magnitudes of groundwater extraction (e.g., OW7, OW14 and OW15). The water-table elevation linearly declined for some observation wells close to the boundary (e.g., OW1, OW5, OW20, OW28 and OW37) for the second category, mostly due to aquifer shrinkage. Finally, the third category comprised conditions where the water table has periodic oscillations and an overall declining elevation trend (e.g., OW3, OW4, OW22, OW32 and OW43). The oscillation is related to seasonal recharge, while over-exploitation caused the substantial long-term drawdown.

Conceptual model

In this section a brief description is given for each conceptual model of the case study, namely the groundwater and surface-water components.

Groundwater conceptual model

A comprehensive and detailed description of the procedure used to develop the groundwater conceptual model of the Neishaboor plain is given by Izady et al. (2014). The method consists of six steps: (1) collection of all available data and information, (2) verification and setup of controlling observations, (3) defining the aquifer geometry, (4) estimation of aquifer hydrodynamic properties, (5) identification of aquifer recharge and discharge, (6) integration of the results from other steps to deliver the overall conceptual model. A brief description of the Neishaboor plain conceptual model is reported here (for more detail, refer to Izady et al. 2014).

The results of a mapping effort using geo-electric sounding (Ministry of Water and Electricity 1966) were used to determine the position of the bedrock. The bedrock depth varies from 0 to 260 m in the different parts of the plain (Fig. 3). A Neogene and marl rock outcrop resides to the east of the plain, which was considered as an impermeable barrier to the groundwater flow system. The deepest section of bedrock, ranging from 180 to 260 m below land surface, resides under the alluvial deposits in the north of the plain. This thick alluvial zone near the mountains is filled with Quaternary and upper Pliocene sediments with great groundwater storage capacity. Also, this region catches mountain runoff via alluvial fans, which is a main source of groundwater recharge—for more detail, refer to the electronic supplementary material (ESM).

Topographic and geologic maps were first employed to define the plain boundary, which was refined using the intersection points of the groundwater level and

Fig. 3 **a** Bedrock-depth contour lines for the Neishaboor aquifer, spatial distribution of sounding points, geo-electric cross sections and boundary conditions (the *red lines* (*A–B* and *C–D*) have inflow boundary conditions, and the *pink line* (*E–F*) has outflow boundary conditions). **b** The geo-electric cross section No. 4 (see Fig. 1 for description of geology) ▶

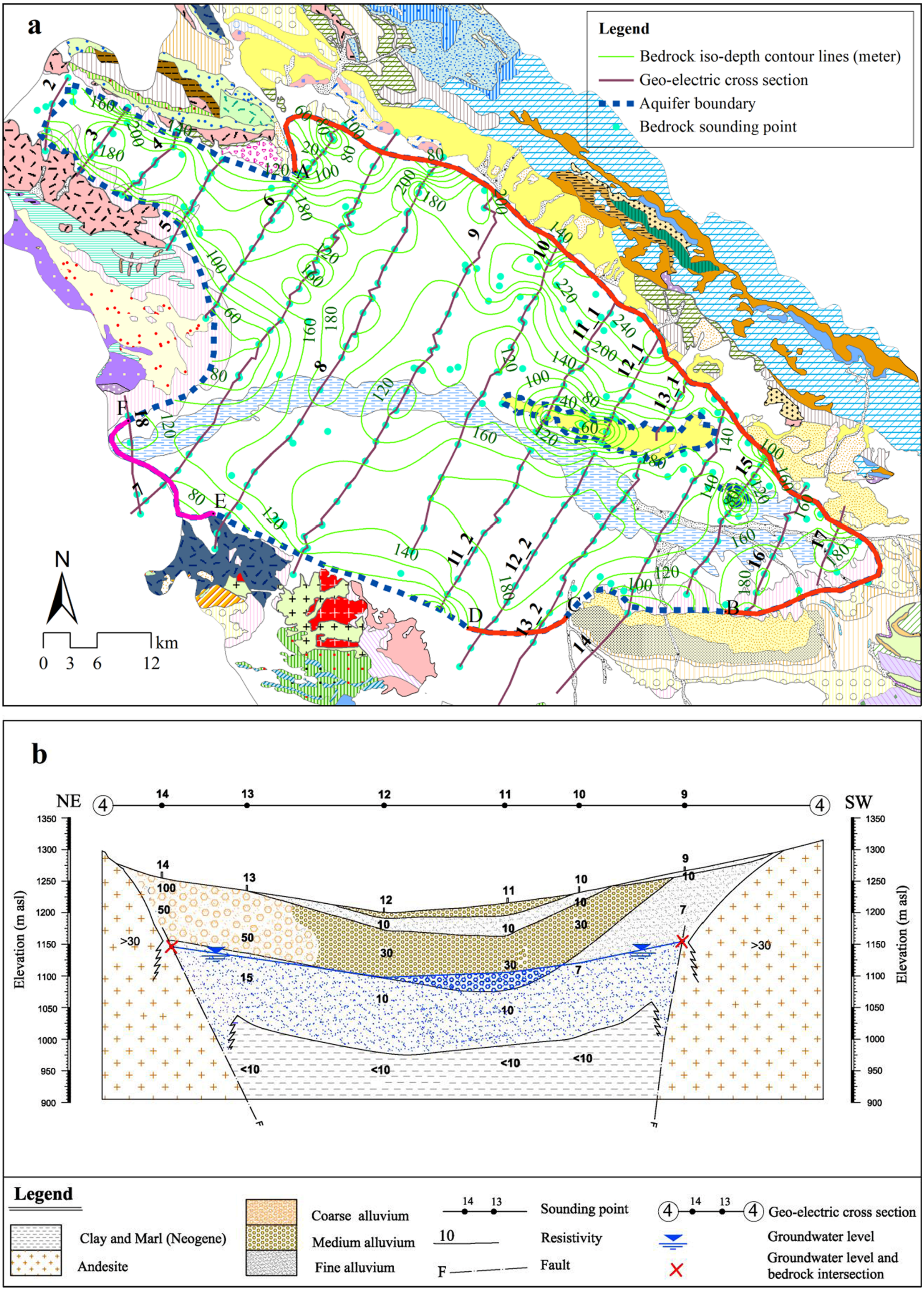
a
Legend
Bedrock iso-depth contour lines (meter)
Geo-electric cross section
Aquifer boundary
Bedrock sounding point
N
0 3 6 12 km
A
B
C
D
E
F
b
NE
SW
Elevation (m asl)
Elevation (m asl)
Legend
Clay and Marl (Neogene)
Andesite
Coarse alluvium
Medium alluvium
Fine alluvium
Sounding point
Resistivity
Fault
Geo-electric cross section
Groundwater level
Groundwater level and bedrock intersection

descending and ascending limbs of the geo-electric cross-sections (see Figures S1–S3 of the ESM). Since the geo-electric cross sections were based on data collected in 1966, and considering that the current groundwater level has declined substantially from that time, the physical aquifer boundaries were modified. This was done by subtracting the bedrock raster from the groundwater level to construct the saturated layer (Fig. 1). The southeast and east boundaries of the aquifer are associated with a groundwater inflow path (Ministry of Water and Electricity 1969). The southeast flow path represents the general direction of flow from the Rokh plain to the Neishaboor plain. The east boundary of the study area is bounded by the Binalood Mountains with low-permeability sedimentary rocks, marl and Neogene materials; however, intervening tributary drainage basins provide a source of groundwater inflow to the study area. The south boundary represents a no-flow condition because of the low permeability of its resident material. The southwest boundary of the study area was characterized as an outflow domain (Fig. 3). The geo-electric survey of 1966, drilling logs, geologic maps and information provided by local consultants all indicate that the Neishaboor aquifer can be considered as an unconfined aquifer.

The spatially distributed hydrodynamic properties were estimated using different methods. Estimated hydraulic conductivity values—ranging from 1.5 to 30 m/day—are larger for the east, south and southwest parts of the plain. However, hydraulic conductivity decreases near the plain's outlet due to fine-grained alluvium. Specific yield exhibits the same trend as hydraulic conductivity. The north and south sections of the plain have the greatest specific yield values (0.169), while the east and west sections are assigned the smallest values (0.05)—for more detail, refer to the ESM.

To determine temporal discharge variations, the results of two consecutive groundwater discharge measurements for 1999 and 2009 were used. Overall, the reported number of wells is 4,003 in 2009, out of which about 2,300 of them were located within the aquifer boundary. It was found that extraction for these wells in 1999 and 2009 were 768 and 681 Mm^3, respectively. Examination of the data reveals that there was a falling discharge trend for the joint wells (13 %); however, 1.7 % of decreased extraction was compensated by an increased number of wells. A linear variation was considered for determining discharge along two consecutive discharge sampling years. The withdrawal for industrial purposes was not taken into consideration, since it is not significant in the investigated area.

In the groundwater conceptual model, it is believed that recharge takes place through four pathways: in fractured rocks in the mountain block with subsequent flow to aquifers; in alluvial fans at the base of the mountains; within streambeds; and via direct infiltration in the plain. Quantification of direct groundwater recharge is a major problem in many water-resource investigations, which is intensified in arid and semi-arid areas, where amounts are low and likely to be lost in the uncertainty of the dominant inputs and outputs for typical water-balance calculations. As mentioned earlier, SWAT was used to estimate recharge by taking into account streamflow and crop yield data sets. Moreover, groundwater extractions for irrigation purposes (as a measure of crop water management) were also considered for calibration.

Surface-water conceptual model

The basic components of a surface-water model are sources and sinks of water, the physical boundaries, land-use and soil maps, and crop management practices in the region. The detail of watershed delineation depends on the spatial accuracy of the digital elevation model (DEM). The Shuttle Radar Topography Mission (SRTM) DEM (grid cell: 90×90) was selected as the base elevation model (Jarvis et al. 2008). The Stream network map produced by the National Cartographic Center (NCC) at a scale of 1:25,000 was cross-checked for conflicting points with satellite images, Google Earth software and field survey and were corrected in some locations. The soil map prepared by Khorasan - Razavi Regional Water Authority at a scale of 1:100,000 and soil data from watershed management and detailed soil reports were employed. The produced map includes 41 types of soil. Soil texture along with soil gradation, rock fragment content, soil saturated hydraulic conductivity and organic carbon content were obtained from the mentioned reports. Other required parameters were estimated using RetC software (van Genuchten et al. 1991). The land use map also prepared by Khorasan-Razavi Regional Water Authority at a scale of 1:100,000 and land use data from detailed watershed management reports were used. The designated land uses consist of 14 main classes: irrigated cropland, dryland cropland, orchard, pasture, range-grasses, range-brush, forest-mixed, forest-evergreen, shrubland, bare ground tundra, wetlands-mixed, sparsely vegetated, residential-medium density and water. Land use in the Neishaboor watershed is predominantly agricultural (47 % of watershed) with the main crops grown in the watershed being irrigated wheat and barley (70 % of the 47 %), sugar beet, cotton, and alfalfa (30 % of the 47 %), followed by rainfed wheat. Records from 23 precipitation, 4 air temperature, and 3 solar radiation gages over a period of 14 years (1997–2010) were used in SWAT (Fig. 1), whereas relative humidity and wind speed was simulated using the weather generator in SWAT. Data were obtained from Khorasan– Razavi Regional Water Authority and Iran Meteorological Organization. Since SWAT is unable to represent the spatial and temporal variability of climate within the basin, a precipitation lapse rate was calculated using mean annual precipitation of the considered gages. The solar radiation was estimated using the Angstrom-Prescott equation (Angstrom 1924), which is an equation with an empirical coefficient that varies for each location. Values of these empirical coefficients were available in the literature (Alizadeh and Khalili 2009)—for more detail about climate data, refer to the ESM. Neishaboor watershed is an irrigated-agriculture-based watershed. Hence, the processes affecting the water balance in an agricultural watershed are highly influenced by crop management; therefore, for the duration of simulation from 1997 to 2012, irrigated and rainfed wheat crops were examined. Typical management data such as cultivated crops, fertilizer application, tillage and harvest operations for different mentioned land uses were collected from several sources. Management operations used for the simulation are given for rainfed and irrigated wheat and corn silage (see Tables S2–S4 in the ESM). The management practices (i.e. planting, harvesting and fertilizer application date and amount) used in this study are based on the average long-term data. Records from five hydrometric gages (Fig. 1) and historical crop yield data collected over a period of 12 years (2000–2012) were used for calibration and validation. It is worth noting that field surveys were conducted to increase the accuracy of collected crop yield data.

Model setup and application

Groundwater and surface water are not isolated components of the hydrologic system, but instead interact in a variety of physiographic and climatic landscapes; thus, development of one commonly affects the other. Therefore, an understanding of the basic principles of interactions between groundwater and surface water is needed for effective management of water resources (Sophocleous 2002). In this study, SWAT and MODFLOW were considered as modeling tools; the model setup and detailed procedure adopted for the combined SWAT-MODFLOW calibration are described in the following sections.

Groundwater flow modeling

MODFLOW (McDonald and Harbaugh 1988), a widely used computer program that simulates three-dimensional (3D) groundwater flow through a porous medium, was used for this study.

Model structure and calibration

Fully transient simulations were conducted for the 2000–2012 period in order to model groundwater flow. Model calibration and validation were carried out for the period of October 2000 to September 2010 and October 2010 to September 2012, respectively. As mentioned earlier, the southeastern and eastern boundary of the aquifer are associated with a groundwater inflow path. There is no information about inflow flux from Mount Binalood through fractured rocks and alluvial fans to the aquifer; therefore, the aquifer boundary was shifted to the first available observation wells and this boundary was named "modeling boundary" (Fig. 1), while the southwest boundary was characterized as an outflow path. For these boundaries, a specific-head-boundary condition was considered (Fig. 4). Monthly measured groundwater level data from the existing observation wells on the model boundary were used to prescribe time-varying constant head boundaries (Fig. 4). As noted, the Neishaboor aquifer is an unconfined aquifer and it was considered as a single layer. The stress period, time step, and time unit was implemented as monthly, monthly, and daily, respectively. A regular mesh and a block centered finite difference grid with 0.25 km^2 cells (500×500 m) with a total of 115 rows and 176 columns was used. Vertically, the model extends from the top of the surface to bedrock level, and varies from 10 to 260 m in different parts of the

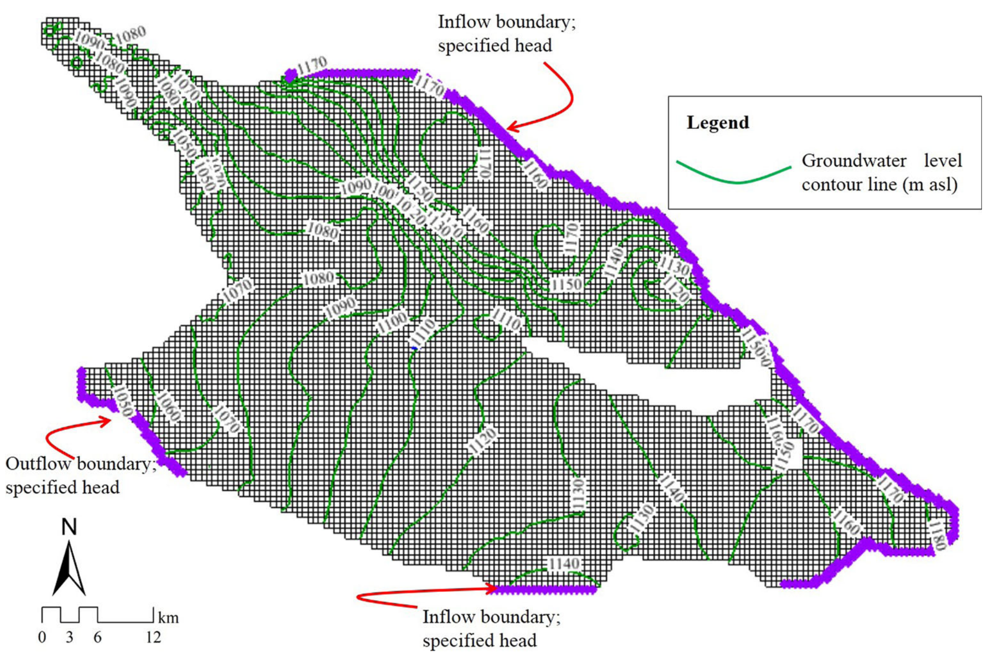

Fig. 4 Finite difference grid with boundary conditions for the Neishaboor plain

plain. With a total grid area of 5,060 km^2, the active model area is 2,360 km^2. The grid was refined near wells with higher extraction rates to facilitate the numerical convergence of model computations in areas of steep hydraulic gradients. The southeast and east boundary of the aquifer associated with a groundwater inflow path. The southwest boundary was also characterized as an outflow path. For these boundaries, specific head boundary condition was considered (Fig. 4).

Based on prepared DEM and bedrock maps, values of the top and bottom elevations were calculated with inverse-distance interpolation method (Tabios and Salas 1985) with a 500×500 cell size. Similarly, the hydraulic conductivity and specific yield were calculated and assigned as initial values in the model. The abstraction values corresponding to all withdrawal wells were considered based on two consecutive discharge sampling events in 1999 and 2009, assuming a linear rate of change in this period. The recharge rates computed by the SWAT were considered as an input for the model. The initial head was obtained from the piezometers and other measured groundwater level of withdrawal wells at October 2000.

Model calibration was accomplished by varying a set of parameters values that aimed at matching simulated groundwater levels with the field observations; the set of parameters included recharge rates, hydraulic conductivity, and specific yield values. The model was initially calibrated by trial and error to understand the response of the model to parameter changes. Afterward, the PEST algorithm (Doherty 1998) was used to achieve optimum calibrations using 48 observation wells as control points. Different criteria were used in order to evaluate the effectiveness of the model and its ability to make predictions for the calibration and validation periods. These included root mean square error (RMSE), normalized RMSE (NRMSE), mean error (ME) and mean absolute error (MAE). NRMSE was employed because the range of groundwater level fluctuation in the calibration and validation periods were different for each observation well, and it seemed that the normalized RMSE value would be more helpful. The NRMSE for whole plain was calculated as follows:

$$\text{Weighted RMSE} = \frac{\sum_{i=1}^{n} RMSE_i \times a_i}{A} \quad (1)$$

$$\text{Weighted drawdown} = \frac{\sum_{i=1}^{n} \Delta h_i \times a_i}{A} \quad (2)$$

$$\text{Normalized RMSE} = \frac{\text{Weighted RMSE}}{\text{Weighted drawdown}} \quad (3)$$

where i refers to the observation well, n is number of observation wells, a is Thiessen area, A is total area, Δh is the difference between maximum and minimum groundwater level fluctuation.

Surface-water modeling

SWAT description

SWAT (Arnold et al. 1998) is a spatially distributed, continuous river watershed scale model developed to predict the impact of land management practices on water, sediment and agricultural chemical yields with varying soils, land use and management conditions over long time periods (Neitsch et al. 2009). Spatial parameterization of the SWAT model is performed by dividing the watershed into sub-watersheds based on topography. These are further subdivided into a series of hydrologic response units (HRU) based on unique soil, land use, and slope characteristics. Main model components consist of climate, hydrology, soil temperature, plant growth, nutrients, pesticides, land management, bacteria, and water routing (Arnold et al. 1998; Gassman et al. 2007; Neitsch et al. 2009). A more detailed description of the model is given by Neitsch et al. (2009)—for more detail about computing groundwater recharge using SWAT, refer to the ESM.

Model structure and calibration

Arc-SWAT version 2009.93.7b (Winchell et al. 2009) was used as an interface for the SWAT program. The simulation period for the Neishaboor surface-water modeling was 1997–2012; the first 3 years were used as a warm-up period to mitigate the impact of the unknown initial conditions and were excluded from the analysis. The Neishaboor watershed was subdivided into 248 subbasins (Fig. 5). To achieve this, a watershed was first delineated using the selected DEM with the smallest possible threshold area (0.008 %). Next, all generated outlets were removed, then new outlets were assigned to SWAT with regard to mountain-plain boundary, horticultural and agricultural farms borders, county boundaries (Fig. 5) and available hydrometric stations limitations. One HRU was considered for each subbasin instead of irregularly distributed HRUs to simplify crop-management data assignments to each subbasin. Constraints for model development are that the area of each subbasin is less than 1 % of the watershed area, and that only one soil type and land use class is dominant for each subbasin. Finally, new subbasins were produced regarding manually assigned outlets. This tedious and time-consuming process was done several times using trial and error with regard to mentioned constraints to obtain appropriate subbasins.

Surface elevation was allowed to vary within each subbasin to account for spatial variability of precipitation and temperature in the watershed, considering orographic effects. The lapse rate values were estimated to be 160 mm/km and 6 °C/km, respectively, and 5 elevation bands were considered in each subbasin. Solar radiation was estimated using the Angstrom-Prescott equation

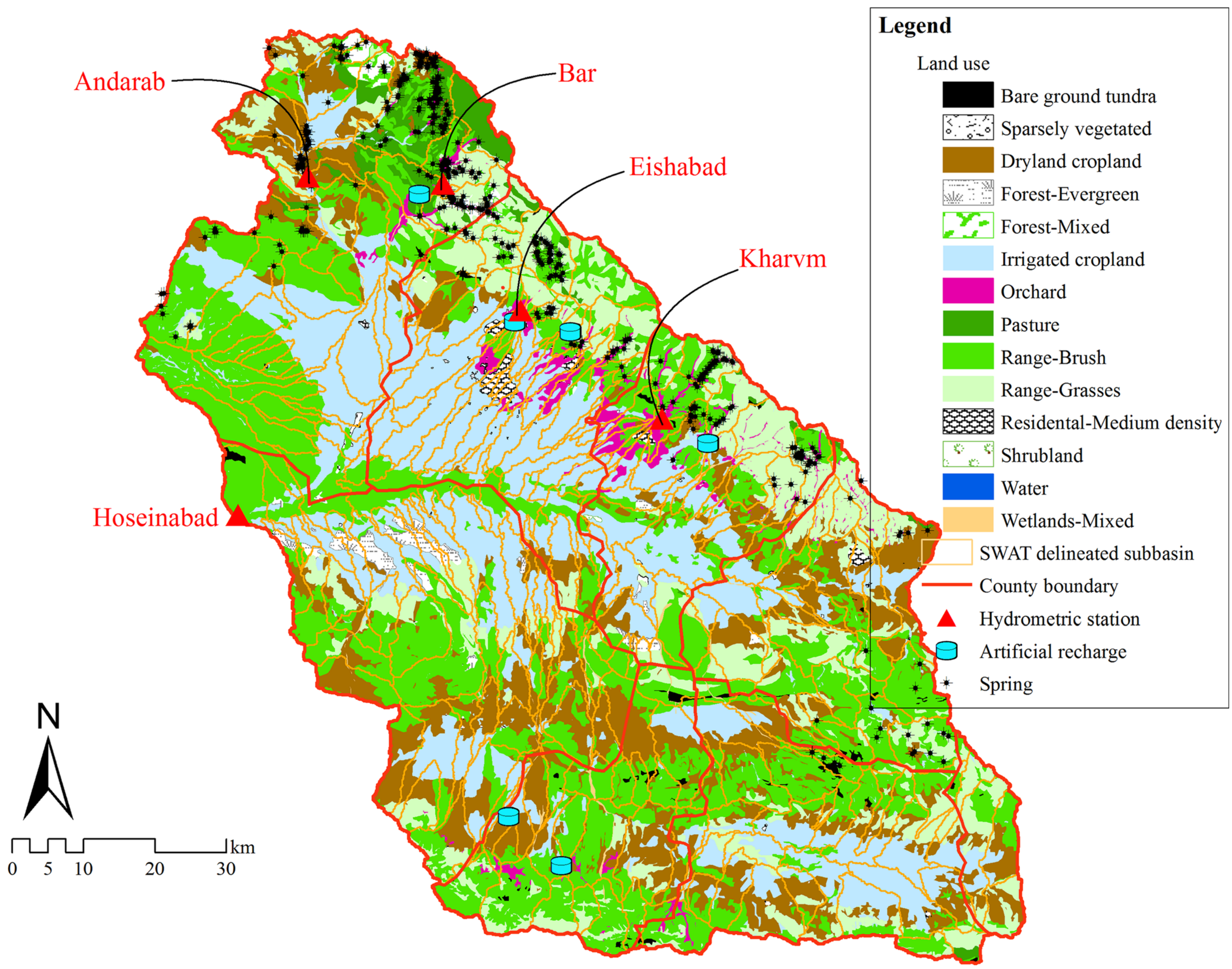

Fig. 5 Land use map of the Neishaboor watershed showing a predominantly agricultural-based watershed along with SWAT delineated subbasins, artificial recharge sites and springs

(Angstrom 1924) in lieu of using the SWAT weather generator because of its influential effect on crop yield (Neitsch et al. 2009). The potential evapotranspiration was computed using the Hargreaves method (Hargreaves and Samani 1982) in which minimum and maximum daily temperature are the only required parameters. Also, the variable storage method was used for channel routing. Manual irrigation method was selected for the crop management. Based on planted crops (irrigated winter wheat and corn silage) and groundwater extraction data, irrigation depths were computed for each subbasin and crop. To calculate irrigation depth, agriculture wells were firstly overlaid on the SWAT delineated subbasins layer. Then, knowing the number of agriculture wells in each subbasin, the total discharge was calculated for each subbasin. Finally, a uniform irrigation rate for each subbasin was estimated by dividing total discharge by subbasin area. Moreover, a depth for each irrigation event was calculated based on each crop's irrigation interval.

The SUFI-2 (Sequential Uncertainty Fitting, ver. 2; Abbaspour 2007) uncertainty analysis algorithm was used for calibration. Methods and data used for model calibration are provided in the ESM—for more detail about *p*-factor, *R*-factor, and NS criteria, refer to the ESM.

Combined SWAT-MODFLOW calibration

SWAT and MODFLOW were iteratively executed to achieve satisfactory results. The procedure adopted for the combined SWAT-MODFLOW calibration is as follows:

1. The initial step was to execute and calibrate SWAT based on all available data and obtained simulated groundwater recharge for each HUR (direct recharge and transmission loss from riverbeds).
2. The groundwater recharge from SWAT's HRUs were reformatted (spatial join between HRU and cells) and fed to MODFLOW cells as the upper boundary condition. Then, MODFLOW was executed and calibrated based on all available data and the adjusted recharge values were extracted from the MODFLOW results.

Table 1 SWAT parameters adjusted during the combined SWAT-MODFLOW calibration and their sensitivity statistics and initial and final values

Parameter[a]	Physical meaning	*t*-value[b]	*p*-value[b]	Initial range	Final range
v__TRNSRCH.bsn	Reach transmission loss	19.92	0.00	(0, 1)	(0.32, 0.57)
r__CN2.mgt	Initial SCS CN II value	18.31	0.00	(−0.5, 0.5)	(−0.42, 0.21)
v__CH_K2.rte	Effective hydraulic conductivity of channel (mm/h)	8.24	0.00	(0, 150)	(35, 47)
v__ALPHA_BF.gw	Baseflow recession constant	3.02	0.00	(0, 1)	(0.3, 0.39)
v__CH_N2.rte	Manning's n value for the main channel	1.63	0.10	(0, 0.3)	(0.19, 0.22)
v__GW_REVAP.gw	"Revap" coefficient	1.50	0.13	(0.02, 0.2)	(0.03, 0.04)
v__SMFMN.bsn	Melt factor for snow on December 21 (mm /°C/day)	1.21	0.23	(0, 10)	(0.21, 2.47)
v__SMTMP.bsn	Snow melt base temperature (°C)	1.16	0.25	(−5, 5)	(−4.21, −2.16)
v__EPCO.hru	Plant uptake compensation factor	0.93	0.35	(0.01, 1)	(0.75, 0.81)
r__SOL_K().sol	Soil hydraulic conductivity (mm/h)	0.90	0.37	(−0.5, 0.5)	(−0.06, 0.06)
v__SLSUBBSN.hru	Average slope length (m)	0.57	0.39	(10, 150)	(34, 43)
v__GW_DELAY.gw	Delay time for aquifer recharge (days)	0.54	0.42	(0, 500)	(471, 484)
v__RCHRG_DP.gw	Aquifer percolation coefficient	0.54	0.44	(0, 1)	(0.3, 0.47)
v__SMFMX.bsn	Melt factor for snow on June 21 (mm /°C/day)	0.45	0.65	(0, 10)	(4.87, 9.48)
r__SOL_BD().sol	Bulk density (g/cm^3)	0.42	0.67	(−0.5, 0.5)	(−0.41, −0.33)
v__SFTMP.bsn	Snowfall temperature (°C)	0.39	0.70	(−5, 5)	(0.27, 3.42)
v__ESCO.hru	Soil evaporation compensation factor	0.35	0.73	(0.01, 1)	(0.72, 0.79)
r__SOL_AWC().sol	Available water capacity	0.20	0.84	(−0.5, 0.5)	(0.23, 0.34)
v__SURLAG.bsn	Surface runoff lag coefficient	0.18	0.85	(1, 24)	(1, 7)
v__TIMP.bsn	Snow pack temperature lag factor	0.15	0.88	(0.01, 1)	(0.06, 0.67)
v__GWQMN.gw	Threshold water level in shallow aquifer for baseflow (mm)	0.14	0.89	(0, 5000)	(2388, 2812)
v__HEAT_UNITS.mgt (Irrigated wheat)	Potential heat units for plant to reach maturity	–	–	(500, 5000)	(2261, 2400)
v__HI_TARG.mgt (Irrigated wheat)	Harvest index target	–	–	(0, 1)	(0.49, 0.57)
r__IRR_AMT.mgt (Irrigated wheat)	Depth of irrigation water applied on HRU	–	–	(−0.5, 0.5)	(−0.28, 0.16)
r__SOL_ZMX.sol	Maximum rooting depth of soil profile			(−0.5, 0.5)	(−0.15, 0.17)
v__HEAT_UNITS.mgt (Rainfed wheat)	–	–	–	(500, 5000)	(2061, 2184)
v__HI_TARG.mgt (Rainfed wheat)	–	–	–	(0, 1)	(0.33, 0.38)

[a] *v* parameter value is replaced by given value or absolute change; *r* parameter value is multiplied by (1+a given value) or relative change (Abbaspour 2007)

[b] *t*-value indicates parameter sensitivity: the larger the *t*-value, the more sensitive the parameter

[c] *p*-value indicates the significance of the *t*-value: the smaller the *p*-value, the less chance of a parameter being accidentally assigned as sensitive

3. The MODFLOW adjusted-recharge values were sent back to SWAT as observed data. The weights for streamflow, crop yield and groundwater extraction were fixed at 1, 0.9 and 0.8, while recharge weight was changed from 0.3 to 0.7 during the iterative executions.
4. Steps two and three (iteration between SWAT and MODFLOW) were repeated to achieve satisfactory results.
5. As a control, computed recharge rates were checked against the independently estimated annual mean groundwater recharge rates. The result of Ahmadi et al. (2014), which were computed based on RIB method (Xu and Beekman 2003), were adopted for the comparison.

Results and discussion

The results of the combined SWAT-MODFLOW modeling are presented in the following sections.

SWAT sensitivity analysis

The sensitivity analysis indicates which processes and their associated parameters in the combined SWAT-MODFLOW primarily control the hydrology of the Neishaboor watershed. Table 1 shows selected SWAT parameters in the calibration process and their sensitivity statistics. The *t*-value provides a measure of sensitivity

Table 2 Model performance statistics for hydrologic calibration and validation periods

Hydrometric station	*p*-factor	*R*-factor	R^2	NS	RMSE (CMS)	NRMSE (%)
Andarab	0.36 (0.22)[a]	1.03 (1.82)	0.61 (0.69)	0.61 (0.59)	0.584 (0.506)[b]	7.8 (6.8)
Kharvm	0.63 (0.74)	0.54 (1.17)	0.66 (0.55)	0.63 (0.47)	0.705 (0.364)	8.8 (4.5)
Hoseinabad (watershed outlet)	0.27 (0.29)	1.68 (2.88)	0.77 (0.51)	0.74 (0.61)	0.923 (0.601)	5.7 (3.7)

[a] Numbers in *parentheses* are validation results

[b] The discharge ranges are 0.0–7.44, 0.0–7.99 and 0.0–16.16 m^3/s for Andarab, Kharvm and Hoseinabad hydrometric stations, respectively

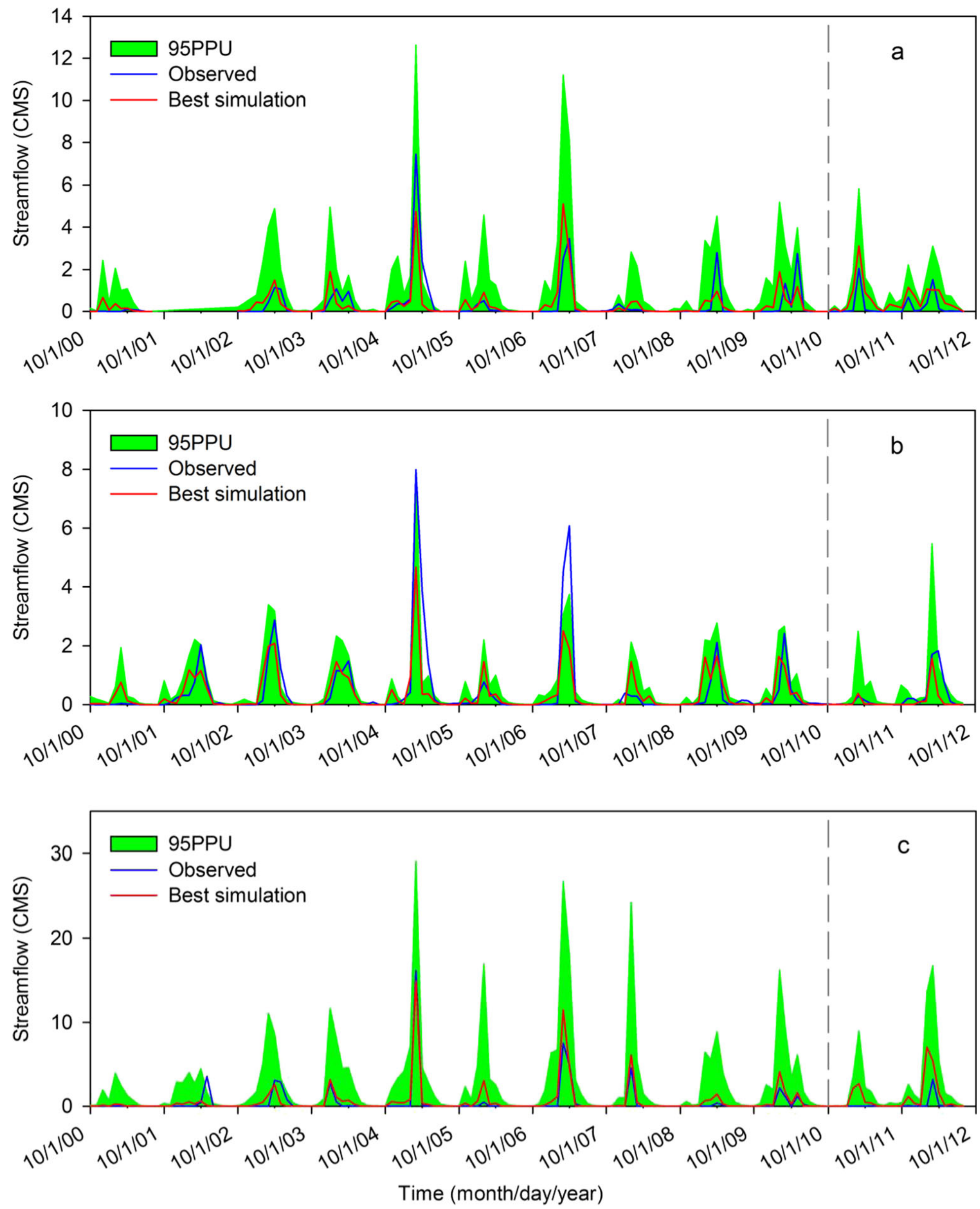

Fig. 6 Plots of observed and simulated mean monthly streamflow during the calibration (Oct. 2000 to Sept. 2010) and validation (Oct. 2010 to Sept. 2012) periods for **a** Andarab, **b** Kharvm, and **c** Hoseinabad hydrometric stations, *95PPU* is the predictive coverage (see definition in the ESM)

(larger values are more sensitive) and *p*-values determine the significance of the parameters (the smaller, the more significant; Abbaspour 2007). The sensitivity analysis resulted in selection of 21 global hydrological parameters (out of 66 parameters) with respect to their sensitivities to streamflow. All crop parameters also were sensitive to crop yield and groundwater extraction.

The reach transmission loss (TRNSRCH) was the most sensitive parameter for the streamflow. Due to the seasonality/flashflood nature of many rivers in semi-arid and arid regions, most of the losses are through streambed infiltration; therefore, runoff is controlled by the reach transmission loss in these regions (Sorman and Abdulrazzak 1993; Scanlon et al. 2002, 2006; de Vries and Simmers 2002; Sophocleous 2005; Wheater 2010; Edmunds 2010). However, as it can be seen from Table 1, the curve number (CN2) was found to be just as sensitive as the reach transmission loss in the Neishaboor watershed, which may be due to the CN's role in rainfall partitioning. The effective hydraulic conductivity and Manning's *n* value mediate infiltration from the streambed. The baseflow recession constant is a direct index of groundwater flow response to changes in recharge. The quantification of the baseflow recession constant is very important in a semi-arid watershed, with low streamflow and quick recession time (Bako and Hunt 1988). Also, snow parameters (melt factor for snow on December 21 and snow melt base temperature) were among the sensitive parameters. The reason for the sensitivities of the snow parameters is that the eastern part of the

Neishaboor watershed is mountainous, and snowmelt controls baseflow in this region.

Hydrologic calibration and uncertainty analysis

Table 1 shows selected SWAT parameters in the combined SWAT-MODFLOW calibration process and their initial and final values, while Table 2 presents calibration statistics for the hydrometric stations. *R*-factor and *p*-factor are representatives of uncertainties in the conceptual model, the parameters, and also the input data. *R*-factors less than 1 generally indicate a good calibration result. While values close to 1 are observed for the stations, the *p*-factor for all stations is relatively small, indicating that the actual uncertainty is likely larger.

The observed and simulated mean monthly streamflow in the calibration and validation periods are shown in Fig. 6. The calibration process was initiated from the upstream gauges—Andarab, Bar, Eishabad and Kharvm—located in the mountainous region of the watershed as well as Hoseinabad, which is located at the watershed outlet (Fig. 5). In the first calibration for the four mountain gauges, SWAT could not predict the base flow except for the Andarab station (Fig 6a) due to the contribution of springs to the base flow (Fig. 5); therefore, the springs were represented in these subbasins as point sources in subsequent simulations. This approach, however, improved the *p*-factor value only for the Kharvm station (Fig. 6b). The question is then, what is the cause of the poor results obtained for the Bar and Eishabad hydrometric stations? The severe elevation variability of these subbasins could be a reason that the few rain gauges employed could not capture the drastic variability of precipitation. Unaccounted-for human activities (e.g., construction of some artificial groundwater recharge sites adjacent to Eishabad and a dam in Bar subbasin that was started in 2003 and completed in 2011) that may affect natural hydrologic processes during the period of study may have also contributed to the poor result. The snow cover at these two subbasins could also influence the model results. SWAT classifies precipitation as rain or snow based on the average daily temperature and snow parameters are not spatially defined (Fontaine et al. 2002). Another reason could be shortcomings of the SCS method. This method cannot simulate runoff from melting snow and on frozen ground. It also does not consider the duration and intensity of precipitation; however, these two precipitation characteristics are necessary for semi-arid watersheds such as the Neishaboor watershed (Maidment 1992). In the end, it was decided to eliminate these hydrometric stations from the calibration period.

After calibrating the Andarab, Kharvm and Hoseinabad stations separately, the entire watershed was calibrated by considering fixed hydrologic parameters for these stations. According to the performance indicators (R^2, NS and RMSE), SWAT simulated the streamflow well, as shown in Table 2. The magnitudes of the correlation statistic (R^2) indicate that reasonable linear correlations exist between the observed and the simulated streamflow for all stations. The NS, which determines the relative magnitude of the residual variance compared to the measured data variance, was in the acceptable range (> 0.5) as suggested by Moriasi et al. (2007). The RMSE statistic, as an accuracy indicator of the overall error, was reasonable, and it can be seen from Fig. 6 that the flow dynamics are simulated quite well for all stations. However, there are significant uncertainties in the peak values on several occasions especially for Andarab and Kharvm mountain stations; specifically, SWAT could not simulate peak discharge in March, April, and May appropriately, which could be due to the reasons aforementioned for the Bar and Eishabad stations. The calibration result was good for the Hoseinabad as a watershed outlet with no/low flow most of the time. The most important reason for achieving satisfactory results is accurate representation of crop management in the watershed, which is related to the fact that evapotranspiration is a major surface-water budget component in arid and semi-arid agricultural-based watersheds, and that considering crop management improves results considerably. The validation results of streamflow are shown in Table 2 and Fig. 6. The *p*-factor and *R*-factor are similar to calibration results indicating consistency in model simulation for the calibration and validation periods.

Crop yield and groundwater extraction calibration and uncertainty analysis

Calibration of a large-scale distributed hydrologic model (9,159 km^2) against streamflow alone may not provide sufficient confidence for all components of the surface-water balance; hence, rainfed/irrigated wheat yield and monthly groundwater extraction data were used to enhance the results. Performance indicators for this part of the study are *R*-factor, RMSE, and NRMSE. Performance indicator values for calibration and validation periods are presented in Table 3. It was observed that SWAT can predict crop yield satisfactorily for irrigated wheat so that *R*-factor and RMSE values were 0.96 and 0.152 t/ha, respectively. Figure 7 shows the observed crop yield against the simulated values. It can be noted that observed yields for irrigated and rainfed wheat were inside or very close to the predicted bands indicating good results. One of the main factors contributing to these robust results for crop yield calibration is the collection of

Table 3 Model performance statistics for annual crop yield calibration and validation periods

Variable	*R*-factor	RMSE (ton/ha)	NRMSE (%)
Irrigated wheat	0.96 (0.57)[a]	0.152 (0.012)[c]	6.9 (0.5)
Rainfed wheat	0.56 (1.16)	0.124 (0.103)	24.8 (22.1)
Groundwater extraction	3.39 (2.90)[b]	2.32 (2.036)	25.4 (22.3)

[a] The crop yield ranges are 1.4–3.6 and 0.145–0.621 t/ha for irrigated and rainfed wheat, respectively

[b] Groundwater extraction range is 15.3–24.4 mm

[c] Numbers in *parentheses* are validation results

information about management practices at the farm scale (e.g., tillage, fertilizer and planting date).

SWAT showed more uncertainty for groundwater extraction compared to the crop yield (Table 3). Figure 8 shows the observed groundwater extraction versus the computed values. The measured groundwater extraction data have greater uncertainty compared to the crop yield data; hence, the simulation results are not expected to be as satisfactory as crop yield. However, as crop yield and groundwater extraction are indicators of spatial "actual evapotranspiration" and "groundwater recharge", their use for calibration improved the simulated outlet streamflow. Indeed, inclusion of these two sets of observed data enhanced overall model performance via better estimation of the model parameters.

The validation results of crop yield and groundwater extraction are also shown in Table 3 and Figs. 7 and 8. Similar results were obtained for both wheat and groundwater extraction in this period, which indicates reliability of the model.

Groundwater flow calibration

The model calibration was carried out for the period Oct. 2000 to Sept. 2010. SWAT-based recharge values were used as an initial input. During the calibration, some of the initial parameter values were modified by trial and error in order to adjust the conceptual model, which was necessary because the conceptual model was initially developed to represent steady-state conditions. To cope with the numerous parameters and large study area, the PEST algorithm (Doherty 1998) was employed for auto-calibration. The calibrated parameters were hydraulic conductivity and specific yield of the aquifer. Figure 9 shows calibrated hydraulic conductivity zoning. Most changes were made for the south and northeast. The greater magnitude of changes for these zones may be due to differences in sediment texture and/or distances from recharge boundaries. Figure 10 shows calibrated specific yield zoning. The zones for which the greatest magnitude of changes occurred are the same as for hydraulic conductivity. After determining the optimum values for hydraulic conductivity and specific yield, recharge values were modified by trial and error to obtain the smallest error for all control points.

The simulated 10-year mean annual estimated combined SWAT-MODFLOW recharge obtained after iteration is presented in Fig. 11. The recharge rate varies from 0 to 960 mm, with an average of 176 mm. This result shows good agreement with the independently determined 10-

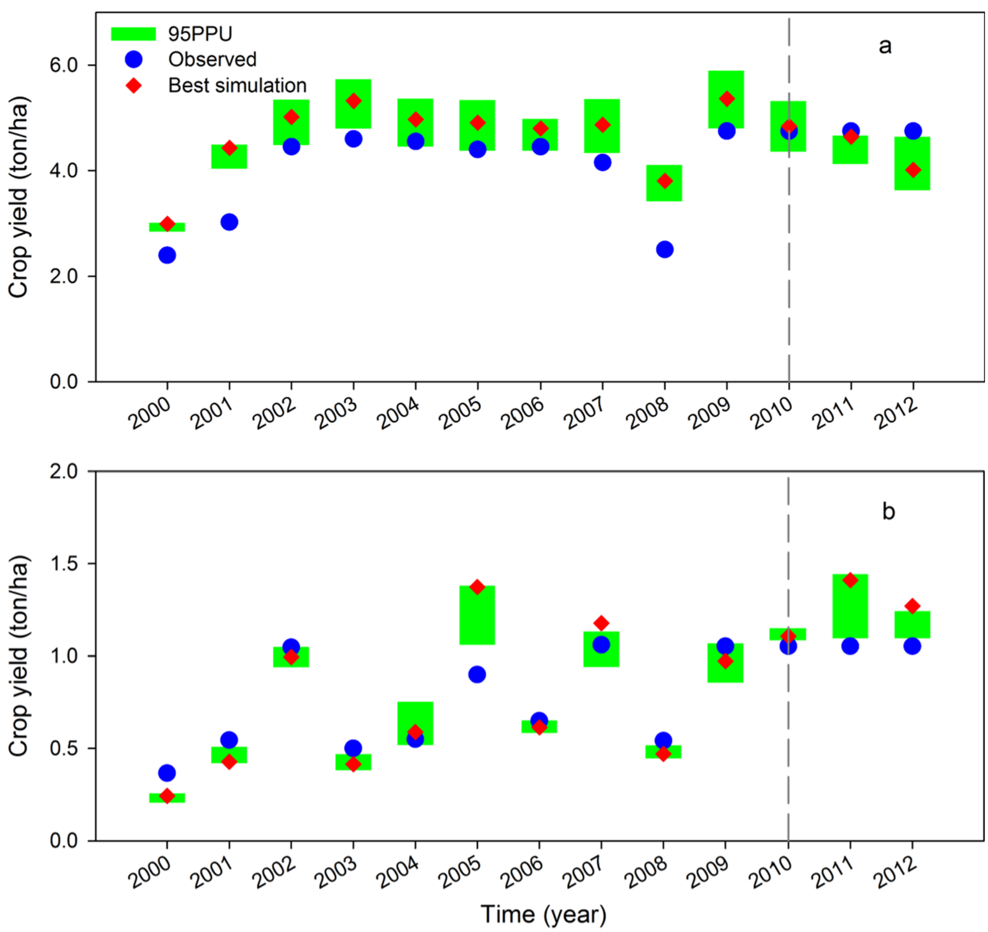

Fig. 7 Plots of observed and simulated annual crop yield during calibration (2000–2010) and validation (2011–2012) period for **a** irrigated wheat and **b** rainfed wheat

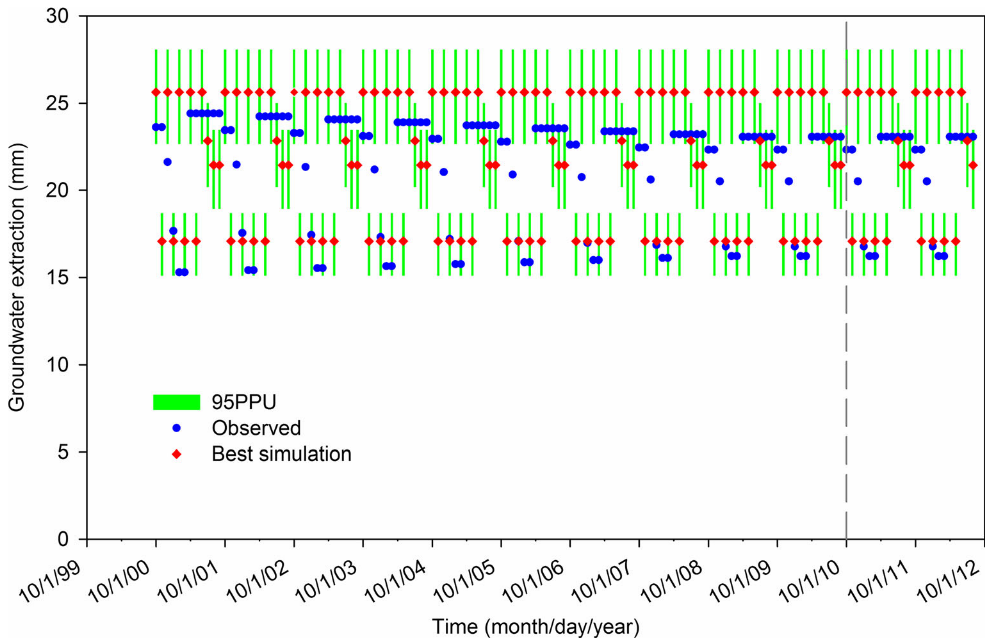

Fig. 8 Plots of observed and simulated groundwater extraction during the calibration (Oct. 2000 to Sept. 2010) and validation (Oct. 2010 to Sept. 2012) periods

year mean annual recharge rate estimated as 160 mm (Ahmadi et al. 2014). The spatial distribution of recharge rate across the study area is consistent with physical conditions. The east and southeast sections of the plain have the greatest amount of recharge. Recharge rates at the Binalood foothills (east part of plain) are high in comparison to other areas within the plain. In this part of the plain, there are many alluvial fans recharging the aquifer; moreover, a vast majority of irrigated land (majority of the agricultural wells) is located in this area and irrigation efficiency is reported to be approximately 40 % for the study area (Khorasan-Razavi Regional Water Authority 2010). Temporal changes in the recharge rate for four representative locations in SWAT-MODFLOW recharge zones (Fig. 11) are presented in Fig. 12. Regions 1 and 4 are both receiving high amounts of recharge from

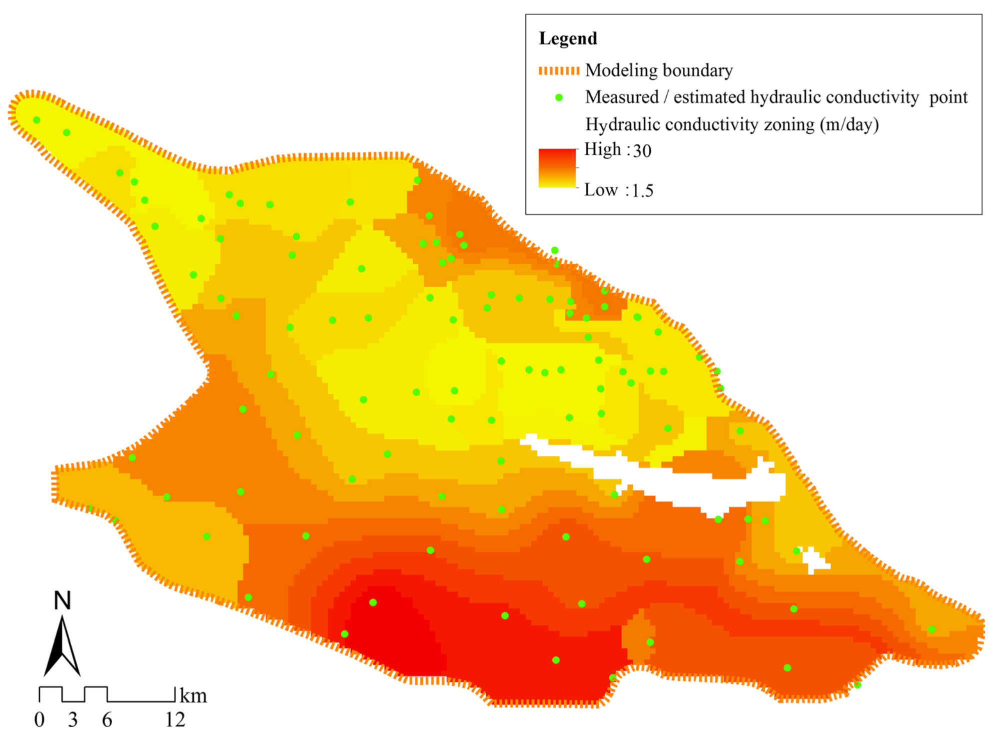

Fig. 9 Hydraulic conductivity zoning within the aquifer and spatial distribution of measured and estimation points

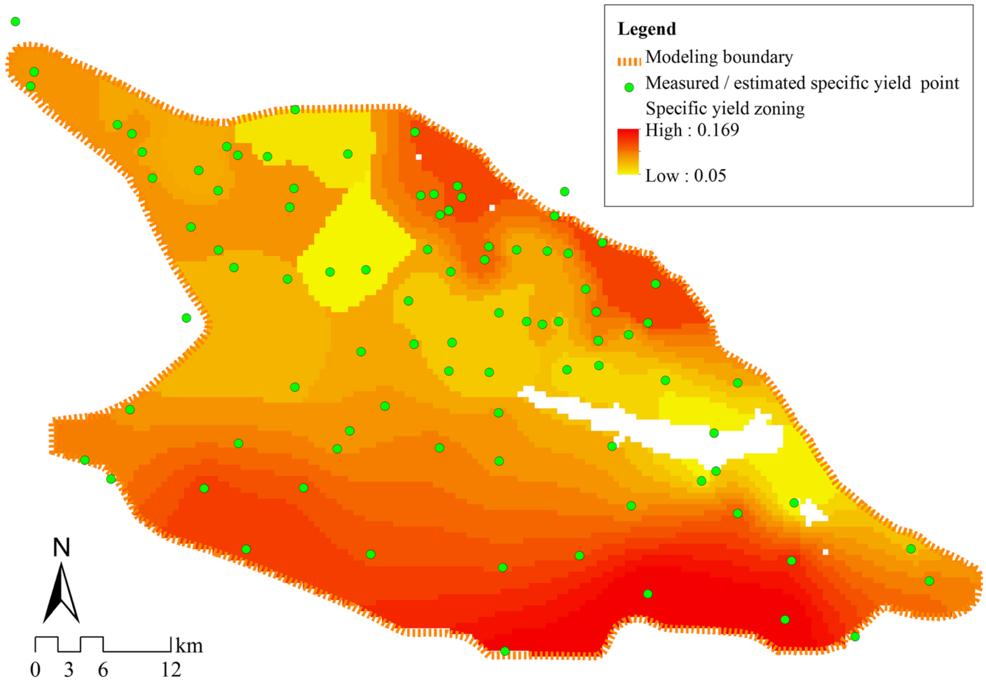

Fig. 10 Specific yield zoning within the aquifer and spatial distribution of measured and estimation points

alluvial fans; however, for region 1 the recharge rate and period are higher and longer. In both cases, recharge starts about early March; probably due to winter precipitation. Regions 2 and 3 are both far from mountainous areas, and their recharge is mostly from irrigation return flows; therefore, recharge starts at the end of spring.

The model performance statistics are given in the Table 4. For the Neishaboor plain, with a total difference in groundwater level on the order of 160 m, a RMSE of 1.75 m is considered quite reasonable. The RMSE was normalized with regard to the groundwater level fluctuations of each observation wells. The result showed that normalized RMSE was almost 15 % during the calibration period for the interior observation wells.

Comparison between computed and measured groundwater levels showed a good match such that 17

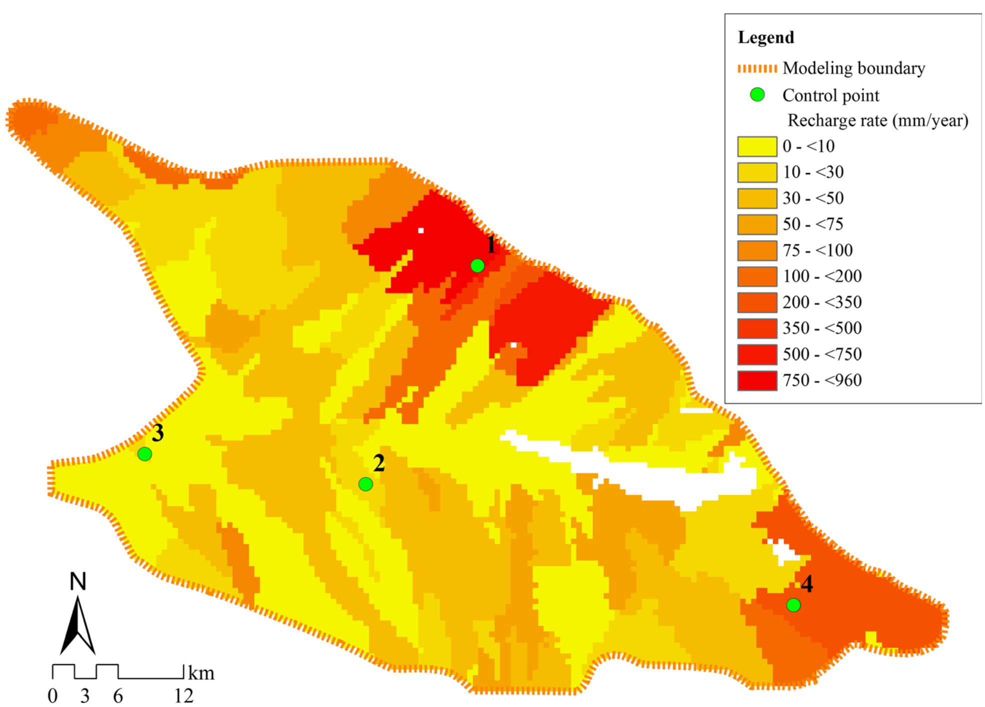

Fig. 11 10-year mean annual recharge estimated using combined SWAT-MODFLOW

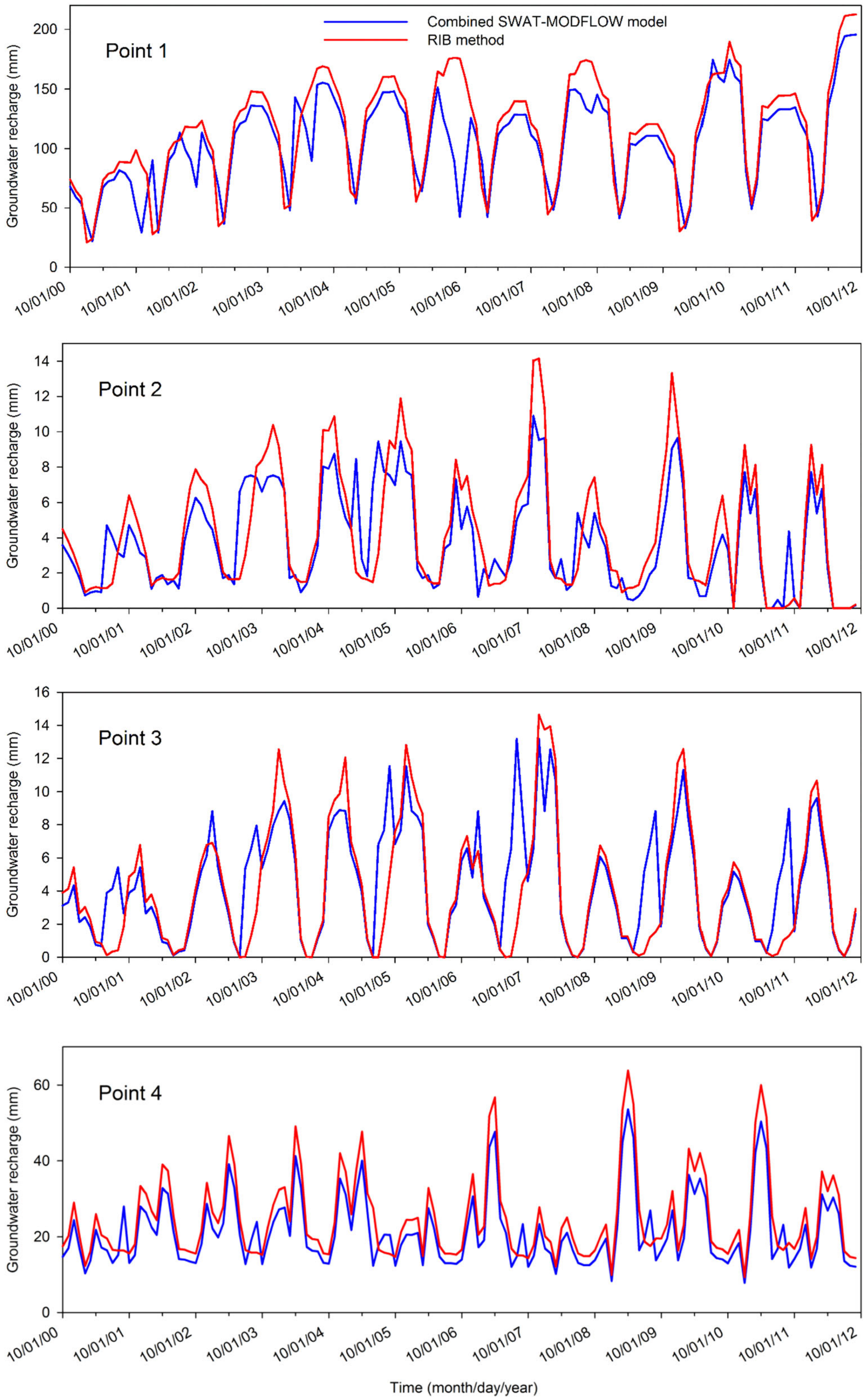

Fig. 12 Plots of 10-year mean annual SWAT-MODFLOW recharge and *RIB method* for four representative points

observation wells from a total of 35 internal observation wells (boundary observation wells were excluded from the analysis) were within 1 m RMSE performance criteria (Fig. 13a). Additionally, 13 of the remainder were within 2 m (Fig. 13b), and 8 others were more than 2 m (Fig. 13c; the results of all observation wells are available in the ESM). Pumping causes a substantial drawdown of the groundwater level in March–June; the end of irrigation

Table 4 Model performance statistics for the calibration and validation periods

Period	ME (m)	MAE (m)	RMSE (m)	NRMSE (%)
Calibration	−0.24	1.112	1.751	15.7
Validation	−0.20	0.982	1.548	73.6

and autumn precipitation subsequently causes a rise in the groundwater level. The good match between computed and observed values under transient conditions gives a better understanding of groundwater dynamics. In fact, such a long period for calibration was chosen to capture the groundwater system dynamics such as seasonal variations and wet/dry period effects.

The observed and computed potentiometric surfaces are shown in Fig. 2. The patterns of observed and computed groundwater levels were quite similar. The RMSE performance criteria along with groundwater level fluctuations of each observation well for the calibration period are also shown in Fig. 2. The spatial distribution of the RMSE is fairly uniform for the interior observation wells which are scattered throughout the entire plain. The worst results are for wells OW15, OW25, OW26, OW32, OW39, OW41, and OW46. These wells are scattered throughout the plain, and not in the vicinity of each other, which suggests the absence of systematic error.

The validation results of control points are shown in Table 4 and Fig. 13. The model performances are similar to the calibration results, indicating consistency of model

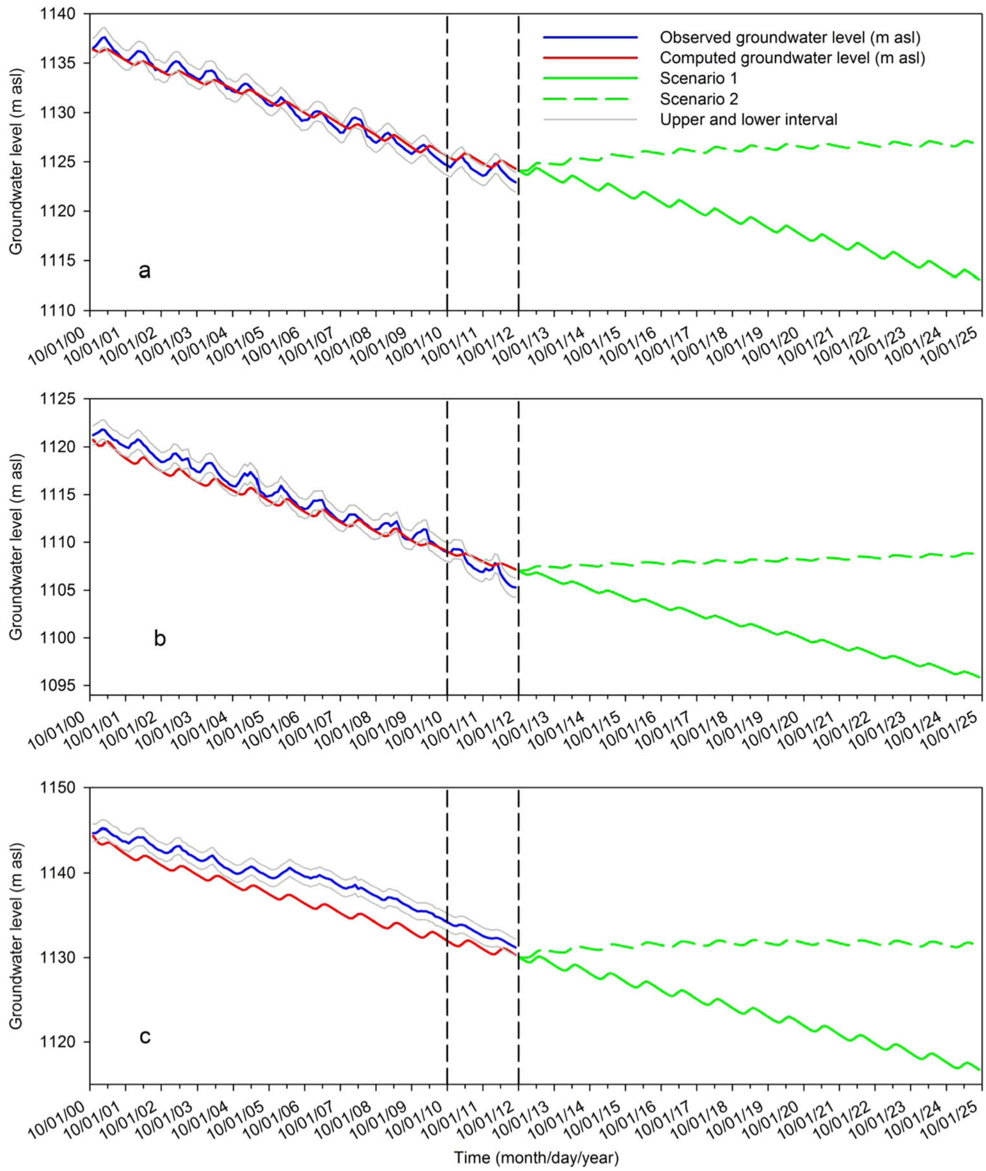

Fig. 13 Plots of observed and computed groundwater levels during the calibration (Oct. 2000 to Sept. 2010), validation (Oct. 2010 to Sept. 2012) and prediction (Oct. 2012 to Sept. 2025) periods for **a** Bagherieh (*OW44*), **b** Arazie Chehl Moghrian (*OW24*) and **c** Arazie Chah Mohandes (*OW39*) observation wells. Note that Bagherieh, Arazie Chehl Moghrian and Arazie Chah Mohandes are examples of observation wells with less than 1, between 1 and 2, and with more than 2-m RMSE performance criteria, respectively. The results for all observation wells were available in the electronic supplementary material (ESM)

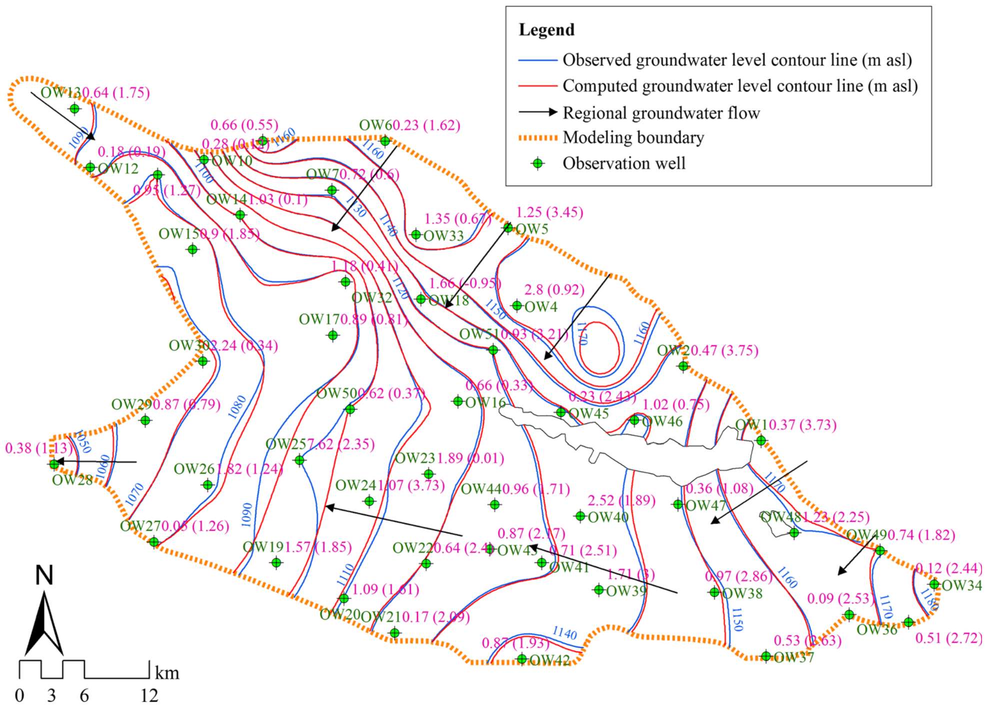

Fig. 14 Observed (*blue line*) and computed (*red line*) groundwater level contour lines for the Neishaboor aquifer (Sept. 2012) along with regional groundwater flow direction (m asl is meter above sea level). The starting date of the validation period is 1 Oct. 2010. Observation well names are given *in green*; numbers beside observation wells (*in purple*) are RMSE performance criteria and groundwater level fluctuation of each observation well (*in parenthesis*; units in meters)

simulation for the calibration and validation periods. The observed and computed potentiometric surfaces of the last stress period of the validation phase (Sept. 2012) along with their RMSE and groundwater level fluctuations of each observation well are shown in Fig. 14. The normalized RMSE was 73 % for the validation period for the interior observation wells, and the weighted average RMSE is less than 1.3 m, which is acceptable regarding the number of observation wells, the model resolution, and the accuracy of water-table data.

Table 5 Annual groundwater balance components in million cubic meters

Period	Groundwater budget component (Mm^3)				
	Inflow		Outflow		Balance
	Q_{in}	Q_R	Q_{out}	Q_E	$\pm\Delta V$
Oct. 2000−Sept. 2001	49	367	33	656	−276
Oct. 2001−Sept. 2002	53	378	28	652	−248
Oct. 2002−Sept. 2003	59	386	25	643	−223
Oct. 2003−Sept. 2004	62	391	25	636	−207
Oct. 2004−Sept. 2005	64	405	26	626	−183
Oct. 2005−Sept. 2006	57	379	29	617	−210
Oct. 2006−Sept. 2007	60	405	28	608	−170
Oct. 2007−Sept. 2008	57	381	30	598	−190
Oct. 2008−Sept. 2009	56	390	33	590	−176
Oct. 2009−Sept. 2010	51	394	35	592	−181
Oct. 2010−Sept. 2011	51	389	34	592	−186
Oct. 2011−Sept. 2012	51	413	35	592	−163
12-year average	56	390	30	617	−201

Groundwater budget components

The annual groundwater components were calculated from October 2000 to September 2012 in a “water year” scale (period between October 1st of one year and September 30th of the next one). The groundwater balance components are as follow:

$$(Q_{\text{in}} + Q_{\text{R}}) + (Q_{\text{out}} + Q_{\text{E}}) = \pm\Delta V \quad (4)$$

where Q_{in} and Q_{out} are the lateral inflow and outflow, respectively, Q_R is the overall recharge (from precipitation, return flow and streambeds), Q_E is the groundwater extraction by pumping and $\pm\Delta V$ is the incremental increase/decrease in groundwater storage. The groundwater and surface-water budget components for the study area are given in Table 5. The areal recharge provides 390 Mm^3/year, while the inflow from the Binalood (east) Mountains and Rokh (south) plain is estimated as 56 Mm^3/year. The lateral groundwater outflow from the study area through the drainage basin is 30 Mm^3/year. Groundwater withdrawal is equivalent to 617 Mm^3/year. The aquifer budget shows a mean annual negative balance (net extraction) of 201 million m^3 due to extensive extraction for agricultural purposes. At current use levels, not accounting for future increases, the Neishaboor aquifer will be depleted in less than 120 years; however, it is possible that induced salinization may cause a decrease in groundwater quality to an unacceptable level many years earlier.

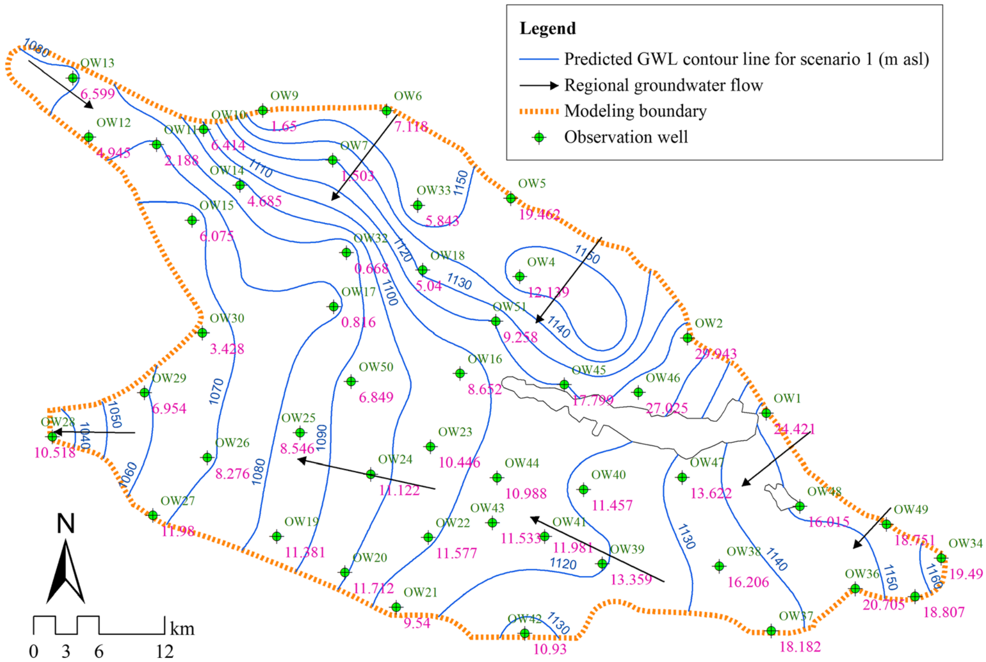

Fig. 15 Predicted groundwater level contour lines (Sept. 2025) along with general groundwater flow direction. The starting date of the simulation period is 1 Oct. 2000. *Numbers close to observation wells* are drawdown values (in meters)

Test management scenarios

Long-term simulations were conducted to examine the impact of two management scenarios on groundwater balance and groundwater level.

Scenario 1: continue the current condition to 2025

The first scenario represents the "no change" case wherein current groundwater use is continued through 2025. A significant drawdown in the groundwater level is simulated for all observation wells as can be seen in Fig. 15. Observation wells located at the east and southeast of the plain exhibited the greatest drawdown (15–30 m) during the scenario period. A total groundwater decline of 10.3 m was forecast, equivalent to 0.8 m/year (Fig. 16). Also, the model boundary at the southeast of the plain shrank because of aquifer desaturation.

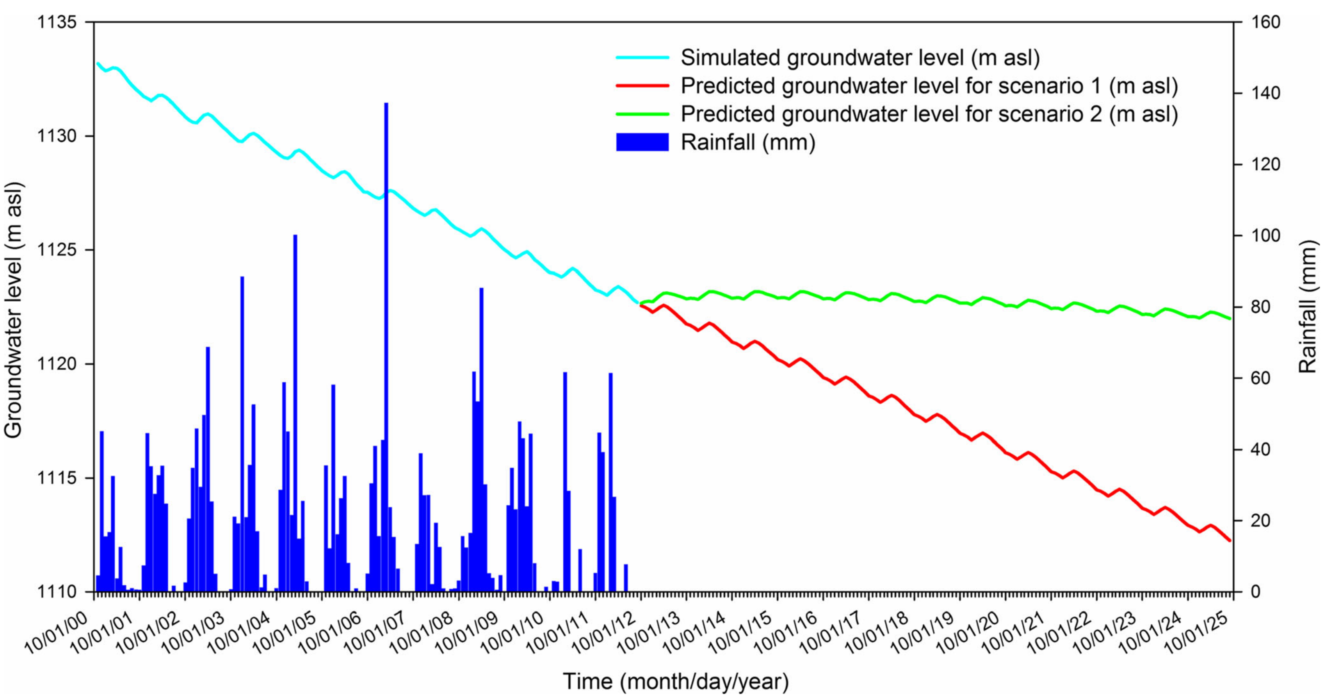

Fig. 16 Predicted groundwater unit hydrograph for scenario 1 (*red line*) and scenario 2 (*green line*)

Scenario 2: achieving the equilibrium condition

This scenario was based on reduced groundwater extraction in order to achieve sustainable yield (Fig. 17). The result showed that groundwater extraction should be decreased by almost 40 % to accomplish this objective. It was assumed that the recharge rates were constant during the prediction years. Also, discharge of all agriculture wells were equally reduced all over the plain. The overall water table rises approximately 0.68 m at the end of the scenario period (September 2025; Fig. 16). Despite achieving overall balance with minimal further decline in aggregate groundwater levels, groundwater levels in the east and southeast part of plain continued to decline; however, the drawdown trend was milder than that of scenario 1. The greatest rise in groundwater level was observed for the center of the plain, which might be due to the fine-grained material and groundwater flow direction.

Summary and conclusion

A numerical model was developed to simulate groundwater flow in the Neishaboor plain. This study provides a significant contribution to the understanding of the groundwater resources in the region, particularly when considering that no prior quantitative analysis had been conducted. The developed model integrates the current knowledge and the hydrogeological information available for the region. It considers all relevant contributions to groundwater flow, including lateral inflow and outflow, as well as recharge and discharge mechanisms. An approach integrating surface and groundwater flow simulations, using a combination of SWAT and MODFLOW, was employed to consider all parameters affecting recharge such as topography, geology, soil, land use, weather, and crop management.

The simulated 10-year mean annual recharge rate varied greatly, ranging from 0 to 960 mm with an average of 176 mm. This result shows good agreement with the independently estimated 10-year mean annual recharge of 160 mm (Ahmadi et al. 2014). Regarding the simulated groundwater budget, the Neishaboor plain shows a mean annual negative balance (net extraction) of 201 million m^3 under the current extensive extraction for agricultural purposes. At current use levels, not accounting for future increases, the Neishaboor aquifer is forecast to be depleted in less than 120 years. The results of scenario testing indicate that groundwater extraction should be decreased by approximately 40 % in order to achieve sustainable yield and stabilize groundwater levels.

Intensive groundwater development in many regions of the world has brought about significant social and economic benefits, but these developments have also resulted in unwanted groundwater depletion and environmental consequences. Groundwater is the main source of water in 54 % of Middle East and North Africa countries. High water stresses are met with groundwater over-abstraction, which is likely to be exacerbated with time with continued population growth and urbanization. In Japan and North China Plain, heavy pumping due to recent agricultural activities has led to groundwater level decline and salt accumulation, respectively. In India, overexploitation has led to problems of salinization and

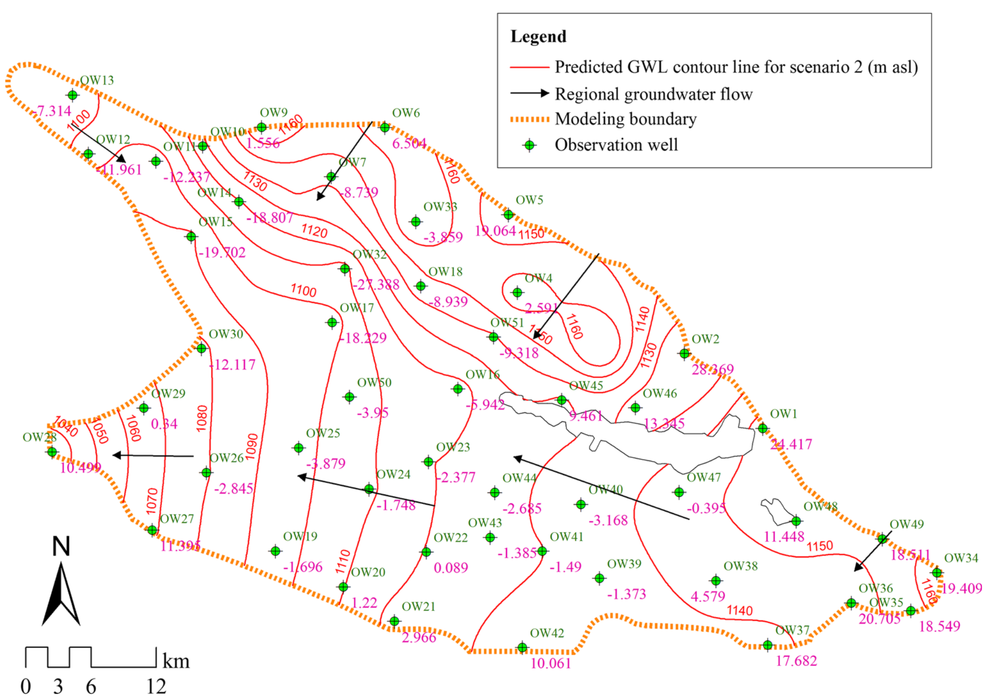

Fig. 17 Predicted groundwater level contour lines (Sept. 2025) along with regional groundwater flow direction. The starting date of the simulation period is 1 Oct. 2000. *Numbers close to observation wells* are drawdown values (in meters); the *minus sign* is for rising groundwater level

pollution of freshwater aquifers, at times even endangering the basic supply of potable water; hence, the urgent need for planning and management of groundwater resources is obvious. The methods used in this study offer a reliable framework for groundwater resources management in the stressed aquifers where interaction between groundwater and surface water is critical. It also can be employed in an irrigated-agriculture-based watershed in which groundwater is a significant source of irrigation. Estimation of groundwater recharge in arid and semi-arid areas is difficult due to the broad range of natural processes influencing groundwater recharge. The integrated groundwater and surface-water modeling approach used herein provides a means by which to produce more robust estimates of spatially distributed groundwater recharge. It is hoped that the lessons learned in this study can help bring about solutions to ensure the sustainability of groundwater resources in other countries which are facing such problems.

Acknowledgements Authors would like to thank Prof. Mary Anderson from the Wisconsin University, Prof. Raghavan Srinivasan from the Texas A&M University, Dr Karim Abbaspour from Swiss Federal Institute of Aquatic Science and Technology (Duebendorf, Switzeland), Dr Il Moon Chung from Korea Institute of Construction Technology (Goyang, Gyeonggi, South Korea), and Dr Sandhya Rao from Indian Institute of Technology (Delhi, India) for their generous help. We also wish to acknowledge the editor Dr Vincent Post, the associate editor Dr Luk Peeters, the technical editorial advisor Sue Duncan and three anonymous reviewers for their constructive comments, which greatly improved the quality of the manuscript.

References

Abbaspour KC (2007) User manual for SWAT-CUP SWAT calibration and uncertainty analysis programs. Swiss Federal Institute of Aquatic Science and Technology, Eawag, Dübendorf, Switzerland

Ahmadi T, Ziaei AN, Rasoulzadeh A, Davary K, Esmaeili K, Izady A (2014) Mapping groundwater recharge areas using CRD and RIB methods in the semi-arid Neishaboor plain. Iran Arab J Geosci. doi:10.1007/s12517-014-1321-2

Alizadeh A, Khalili N (2009) Estimation of angstrom coefficient and developing a regression equation for solar radiation estimation (case study: Mashhad) (in Persian). J Water Soil 23(1):229–238

Allison GB, Barnes CJ, Hughes MW, Leany IWJ (1984) Effects of climate and vegetation on oxygen-18 and deuterium profiles in soils. In: Isotope hydrology. International Atomic Energy Agency, Vienna, pp 105–123

Angstrom A (1924) Solar and terrestrial radiation. Q J Roy Meteorol Soc 50:121–126

Arnold JG, Srinivasan R, Muttiah RS, Williams JR (1998) Large area hydrologic modeling and assessment, part 1: model development. J Am Water Resour Assoc (JAWRA) 34:73–89

Bako MD, Hunt DN (1988) Derivation of baseflow recession constant using computer and numerical analysis. Hydrol Sci J 33(4):357–367

Bedekar V, Niswonger RG, Kipp K, Panday S, Tonkin M (2012) Approaches to the simulation of unconfined flow and perched groundwater flow in MODFLOW. Ground Water 187–198

Bejranonda W, Koontanakulvong S, Koch M (2007) Surface and groundwater dynamic interactions in the upper Great Chao Phraya plain of Thailand: semi-coupling of SWAT and MODFLOW. In: Groundwater and ecosystems, IAH Selected Papers on Hydrogeolgy, IAH, Goring, UK, pp 17–21

Bredehoeft J, Hall P (1995) Ground-water models. Ground Water 33:530–531

De Vries JJ, Simmers I (2002) Groundwater recharge: an overview of processes and challenges. Hydrogeol J 10:5–17

Doherty J (1998) PEST: model independent parameter estimation, user's manual. Watermark, Brisbane, Australia

Doherty J, Simmons C (2013) Groundwater modelling in decision support: reflections on a unified conceptual framework. Hydrogeol J 21:1531–1537

Edmunds WM (2010) Conceptual models for recharge sequences in arid and semi-arid regions using isotopic and geochemical methods. In: Wheater HS, Mathias SA, Li X (eds) Groundwater modeling in arid and semi-arid areas. Cambridge Univ. Press, Cambridge, pp 21–38

FAO, Food and Agriculture Organization (1986) Yield response to water. In: Irrigation and Drainage Paper 33. FAO, Rome

Fontaine TA, Cruickshank TS, Arnold JG, Hotchkiss RH (2002) Development of a snowfall-snowmelt routine for mountainous terrain for the soil water assessment tool (SWAT). J Hydrol 262 (1–4):209–223

Gassman PW, Reyes MR, Green CH, Arnold JG (2007) The soil and water assessment tool historical development, applications, and future research directions. Trans ASABE 50(4):1211–1250

Ghahraman B (2006) Time trend in the mean annual temperature of Iran. Turk J Agric For 30:439–448

Ghahraman B, Taghvaeian S (2008) Investigation of annual rainfall trends in Iran. J Agric Sci Technol 10:93–97

Gieske ASM (1992) Dynamics of groundwater recharge: a case study in semi-arid eastern Botswana. PhD Thesis, Vrije Universiteit, Amsterdam, 289 pp

Hargreaves GH, Samani ZA (1982) Estimating potential evapotranspiration. J Irrig Drain Div 108(3):225–230

Herczeg AL, Leaney FW (2011) Review: environmental tracers in arid-zone hydrology. Hydrogeol J 19:17–29

Hoseini A, Farajzadeh M, Velayati S (2005) The water crisis analysis in Neishaboor plain with considering environmental planning (in Persian). Khorassan-Razavi Regional Water Company, Mashhad, Iran

Izady A, Davary K, Alizadeh A, Ghahraman B, Sadeghi M, Moghaddamnia A (2012) Application of panel-data modeling to predict groundwater levels in the Neishaboor Plain, Iran. Hydrogeol J 20(3):435–447. doi:10.1007/s10040-011-0814-2

Izady A, Davary K, Alizadeh A, Moghaddam Nia A, Ziaei AN, Hasheminia SM (2013) Application of NN-ARX model to predict groundwater level in the Neishaboor Plain, Iran. Water Resour Manag 27:4773–4794. doi:10.1007/s11269-013-0432-y

Izady A, Davary K, Alizadeh A, Ziaei AN, Alipoor A, Joodavi A, Brusseau ML (2014) A framework toward developing a groundwater conceptual model. Arab J Geosci 7:3611–3631. doi:10.1007/s12517-013-0971-9

Jarvis A, Reuter HI, Nelson A, Guevara E (2008) Hole-filled SRTM for the globe Version 4, available from the CGIAR-CSI SRTM 90 m Database. http://srtm.csi.cgiar.org. Accessed December 2014

Jensen ME (1968) Water consumption by agricultural plants. In: Water deficits in plant growth, vol 1. Academic, New York, pp 1–22

Khorasan-Razavi Regional Water Authority (2010) Water resources study of the Neishaboor watershed report (in Persian). In: Integrated study and water budget, vol 4. Ministry of Energy, Tehran

Kim NW, Chung IM, Won YS, Arnold JG (2008) Development and application of the integrated SWAT-MODFLOW model. J Hydrol 356:1–16

Lerner DN, Issar AS, Simmers I (1990) Groundwater recharge: a guide to understanding and estimating natural recharge. IAH Int Contrib Hydrogeol, vol 8. Heise, Hanover, Germany, 345 pp

Llamas MR, Custodio E (eds) (2002) Intensive use of groundwater: challenges and opportunities. CRC, Boca Raton, FL

Maidment DR (1992) Handbook of hydrology. McGraw-Hill, Co., New York

McDonald MG, Harbaugh AW (1988) A modular three dimensional finite-difference ground-water flow model. US Geol Surv Tech Water Resour Invest, book 6. US Geological Survey, Reston, VA

Ministry of Water and Electricity (1966) Etude géophysique par prospection électrique, Dans la region de NECHABOUR [Geophysical study of the Neishaboor region using Geo-electric method]. Groundwater Department, Division of Water Resources, Ministry of Water and Electricity, Tehran, Iran

Ministry of Water and Electricity (1969) Neishaboor aquifer assessment report (in Persian). Ministry of Water and Electricity, Tehran, Iran

Moriasi DN, Arnold JG, Van Liew MW, Bingner RL, Harmel RD, Veith TL (2007) Model evaluation guidelines for systematic quantification of accuracy in watershed simulations. Trans ASABE 50(3):885–900

Nair SS, King KW, Witter JD, Sohngen BL, Fausey NR (2011) Importance of crop yield in calibrating watershed water quality simulation tools. J Am Water Resour Assoc (JAWRA) 47(6):1285–1297

Neitsch SL, Arnold JG, Kiniry JR, Williams JR, King KW (2009) Soil and water assessment tool. In: Theoretical documentation, version 2009. TWRI TR-191, College Station, TX

Scanlon BR, Healy RW, Cook PG (2002) Choosing appropriate techniques for quantifying groundwater recharge. Hydrogeol J 10:18–39. doi:10.1007/s10040-0010176-2

Scanlon BR, Keese KE, Flint AL, Flint LE, Gaye CB, Edmunds WM, Simmers I (2006) Global synthesis of groundwater recharge in semiarid and arid regions. Hydrol Process 20(15):3335–3370

Sophocleous M (2002) Interactions between groundwater and surface water: the state of the science. Hydrogeol J 10(1):52–67

Sophocleous MA (2005) Groundwater recharge and sustainability in the High Plains aquifer in Kansas, USA. Hydrogeol J 13(2):351–365

Sophocleous MA, Perkins SP (2000) Methodology and application of combined watershed and ground water models in Kansas. J Hydrol 236(3–4):185–201

Sophocleous MA, Koelliker JK, Govindaraju RS, Birdie T, Ramireddygari SR, Perkins SP (1999) Integrated numerical modeling for basin wide water management: the case of the Rattlesnake Creek basin in south central Kansas. J Hydrol 214(1–4):179–196

Sorman AU, Abdulrazzak MJ (1993) Infiltration-recharge through wadi beds in arid regions. Hydrol Sci J 38(3):173–186

Srinivasan R, Zhang X, Arnold J (2010) SWAT ungauged: hydrological budget and crop yield predictions in the upper Mississippi River Basin. Trans ASABE 53(5):1533–1546

Sun H, Cornish PS (2005) Estimating shallow groundwater recharge in the headwaters of the Liverpool Plains using SWAT. Hydrol Process 19(3):795–807

Tabios GQ, Salas JD (1985) A comparative analysis of techniques for spatial interpolation of precipitation. J Am Water Resour Assoc 21(3):365–380

van Genuchten M, Leij F, Yates S (1991) The RETC code for quantifying the hydraulic functions of unsaturated soils. Technical Report EPA/600/2-91/065, US Environmental Protection Agency, Washington, DC

Velayati S, Tavassloi S (1991) Resources and problems of water in Khorasan province (in Persian). Astan Ghods Razavi, Mashhad

Wheater HS (2010) Hydrological processes, groundwater recharge and surface-water/groundwater interactions in arid and semi-arid areas. In: Wheater HS, Mathias SA, Li X (eds) Groundwater modeling in arid and semi-arid areas. Cambridge Univ Press, Cambridge, UK, pp 5–37

Winchell M, Srinivasan R, Di Luzio M, Arnold JG (2009) ArcSWAT Interface for SWAT2005: user's guide. Blackland Research Center, Texas Agricultural Station and Grassland, Soil and Water Research Laboratory, USDA Agricultural Research Service, Temple, TX

Xu Y, Beekman HE (eds) (2003) Groundwater recharge estimation in Southern Africa. UNESCO IHP Series, No. 64, UNESCO Paris